

Parametric bootstrap inference for stratified models with high-dimensional nuisance specifications

Ruggero Bellio^{*1}, Ioannis Kosmidis^{†2, 3}, Alessandra Salvan^{‡4}, and Nicola Sartori^{§4}

¹Department of Economics and Statistics, University of Udine, Udine, 33100, Italy

²Department of Statistics, University of Warwick, Coventry, CV4 7AL, UK

³The Alan Turing Institute, London, NW1 2DB, UK

⁴Department of Statistical Sciences, University of Padova, 35121, Padova, Italy

November 2, 2020

Abstract

Inference about a scalar parameter of interest typically relies on the asymptotic normality of common likelihood pivots, such as the signed likelihood root, the score and Wald statistics. Nevertheless, the resulting inferential procedures have been known to perform poorly when the dimension of the nuisance parameter is large relative to the sample size and when the information about the parameters is limited. In such cases, the use of asymptotic normality of analytical modifications of the signed likelihood root is known to recover inferential performance. It is proved here that parametric bootstrap of standard likelihood pivots results in as accurate inferences as analytical modifications of the signed likelihood root do in stratified models with stratum specific nuisance parameters. We focus on the challenging case where the number of strata increases as fast or faster than the stratum samples size. It is also shown that this equivalence holds regardless of whether constrained or unconstrained bootstrap is used. This is in contrast to when the dimension of the parameter space is fixed relative to the sample size, where constrained bootstrap is known to correct inference to higher-order than unconstrained bootstrap does. Large scale simulation experiments support the theoretical findings and demonstrate the excellent performance of bootstrap in some extreme modelling scenarios.

Keywords: *incidental parameters; modified profile likelihood; two-index asymptotics; profile score bias*

1 Introduction

Standard likelihood inference about a scalar parameter of interest is based on the asymptotic normality of likelihood pivots, such as the signed likelihood root, score and Wald statistics. This asymptotic approximation can be quite inaccurate in the presence of many nuisance parameters. An alternative, which guarantees higher accuracy, is based on the asymptotic normality of an analytical modification of the signed likelihood root, termed modified signed likelihood root (see for instance [Severini, 2000](#), Chapter 7). In a two-index stratified asymptotic setting, in which both the dimension of the data and the number of nuisance parameters grow, the modified

*ruggero.bellio@uniud.it

†ioannis.kosmidis@warwick.ac.uk

‡alessandra.salvan@unipd.it

§nicola.sartori@unipd.it

signed likelihood root has been proved to be highly accurate even in rather extreme scenarios with many nuisance parameters and very limited information (Sartori, 2003).

Parametric bootstrap methods provide an alternative assessment of tail probabilities for likelihood pivots and, in standard asymptotic settings, where the number of nuisance parameters is fixed and regularity conditions are satisfied (Severini, 2000, Section 3.4), have been shown to guarantee the same level of asymptotic accuracy as analytical modifications of the signed likelihood root (see Young and Smith, 2005, Chapter 11). In particular, the two main variants of parametric bootstrap are constrained or unconstrained bootstrap (also known as conventional bootstrap). In the latter, the sampling distribution of the statistic is computed at the full maximum likelihood estimate, and in the former at the constrained maximum likelihood estimate for a given value of the parameter of interest. In standard asymptotic settings, constrained bootstrap (DiCiccio et al., 2001; Lee and Young, 2005) corrects inference about a scalar parameter in the presence of nuisance parameters to higher order than unconstrained bootstrap. Although bootstrap methods are, typically, more computationally demanding than analytical approximations to the distribution of pivots, they are available in some non-regular cases in which the modified signed likelihood root is not computable.

We investigate the properties of parametric bootstrap in models for stratified data in a two-index asymptotic setting, where both the number q of strata and the sample size m of each stratum grow. In this scenario, the aim of higher-order solutions is to recover first-order validity of inferential procedures when standard first-order results are typically no longer valid due to the presence of high-dimensional nuisance specifications. In particular, the usual likelihood pivots are asymptotically standard normal provided $q = o(m)$, while the condition for the modified directed deviance is $q = o(m^3)$ (Sartori, 2003). If $q = O(m^\alpha)$, then for $0 \leq \alpha < 1$ the asymptotic normality of standard likelihood pivots still holds. For this reason, we focus our attention on the highly stratified case with $\alpha \geq 1$ where asymptotic normality fails. We show here that accuracy of parametric bootstrap inference is ensured provided that $\alpha < 3$. The same order of error is obtained both with constrained and unconstrained bootstrap, which is in contrast to standard asymptotic settings. On the other hand, when $\alpha \geq 1$ the aim is to recover first-order accuracy and in such setting both variants of parametric bootstrap are as accurate as higher-order analytical solutions. The theoretical results are supported by extensive simulation studies³, which illustrate that parametric bootstrap is at least as accurate as use of the modified signed likelihood root, and provide evidence that it can be even more accurate in some very extreme scenarios.

2 Likelihood inference

Let $l(\theta) = l(\theta; y)$ be the log-likelihood function for a parameter θ based on a sample y of size n . We consider the case where the vector of parameters is partitioned as $\theta = (\psi, \lambda^\top)^\top$, where ψ is a scalar parameter of interest and λ is a vector of nuisance parameters, and denote by $\hat{\theta} = (\hat{\psi}, \hat{\lambda}^\top)^\top$ the maximum likelihood estimate of θ and by $\hat{\theta}_\psi = (\psi, \hat{\lambda}_\psi^\top)^\top$ the constrained maximum likelihood estimate of θ for fixed ψ . We let $U(\theta) = \nabla l(\theta)$ denote the score vector, with $U(\theta) = (U_\psi(\theta), U_\lambda(\theta)^\top)^\top$. Moreover, $j(\theta) = -\nabla \nabla^\top l(\theta)$ is the observed information and $i(\theta) = E_\theta\{j(\theta)\}$ is the expected information. The argument θ will be dropped when no ambiguity arises. Blocks will be denoted by subscripts, as in $U_\psi = U_\psi(\theta)$, $U_\lambda = U_\lambda(\theta)$, $i_{\psi\psi} = i_{\psi\psi}(\theta)$, $i_{\psi\lambda} = i_{\psi\lambda}(\theta)$, and so on.

The signed likelihood root, the score statistic and Wald statistic for inference about ψ are

$$R(\psi) = \text{sign}(\hat{\psi} - \psi) \sqrt{2 \left\{ l(\hat{\theta}; y) - l(\hat{\theta}_\psi; y) \right\}} \quad (1)$$

$$S(\psi) = \frac{U_p(\psi)}{\sqrt{i_{\psi\psi \cdot \lambda}(\hat{\theta}_\psi)}}, \quad (2)$$

$$T(\psi) = (\hat{\psi} - \psi) \sqrt{j_p(\hat{\psi})}, \quad (3)$$

respectively, where $U_p(\psi) = U_\psi(\hat{\theta}_\psi)$ is the profile score, $j_p(\psi) = -dU_p(\psi)/d\psi$ is the profile observed information and $i_{\psi\psi \cdot \lambda} = i_{\psi\psi} - i_{\psi\lambda} i_{\lambda\lambda}^{-1} i_{\lambda\psi}$ is the partial information about ψ .

Computation of p -values and confidence intervals for ψ requires the distribution of statistics (1), (2) and (3). In standard asymptotic settings, one possibility, is to rely on the first-order asymptotic normal approximation to the distribution of (1), (2) and (3). For instance, $\text{pr}_\theta\{R(\psi) \leq R(\psi)^{obs}\} = \Phi(R(\psi)^{obs})\{1 + O(n^{-1/2})\}$, where $\Phi(\cdot)$ denotes the standard normal distribution function and the superscript *obs* is used to denote evaluation at the observed data. Improved accuracy can be obtained with higher-order modifications $R^*(\psi)$ of $R(\psi)$, such that $\text{pr}_\theta\{R(\psi) \leq R(\psi)^{obs}\} = \Phi(R^*(\psi)^{obs})\{1 + O(n^{-1})\}$. [Barndorff-Nielsen \(1986\)](#) developed a modified signed likelihood root $R^*(\psi)$ which is standard normal with error of order $O(n^{-3/2})$. Following this seminal work, there have been various alternative versions of $R^*(\psi)$ (see [Pierce and Bellio, 2017](#), for an accessible overview).

An alternative to the asymptotic approximations to the distribution of (1), (2) and (3) is parametric bootstrap, which provides approximations for p -values, such as $\text{pr}_\theta\{R(\psi) \leq R(\psi)^{obs}\}$, with error of order $O(n^{-1})$. There are two main variants of parametric bootstrap: i) unconstrained bootstrap where samples are simulated from the model at $\hat{\theta}^{obs}$, and ii) constrained bootstrap where samples are simulated at $\hat{\theta}_\psi^{obs}$ (see [DiCiccio et al., 2001](#); [Lee and Young, 2005](#); [Young and Smith, 2005](#), Chapter 11).

In standard asymptotic settings, unconstrained bootstrap provides second-order accuracy. If data y^k are simulated from the model with parameter $\hat{\theta}^{obs}$, ($k = 1, \dots, K$), then p -values for (1) calculated as

$$\hat{p}_1^R(\psi) = \frac{1}{K} \sum_{k=1}^K I\{R(\hat{\psi}^{obs})^k \leq R(\psi)^{obs}\} \quad (4)$$

are uniform on $(0, 1)$ under repeated sampling with error of order $O(n^{-1})$. In (4), $I\{\cdot\}$ is the indicator function and $R(\hat{\psi}^{obs})^k$ is the signed likelihood root of the k th bootstrap sample, evaluated at $\hat{\psi}^{obs}$. In contrast, constrained bootstrap provides third order accuracy; if data y^k are simulated at $\hat{\theta}_\psi^{obs}$, $k = 1, \dots, K$, p -values for (1) calculated as

$$\hat{p}_2^R(\psi) = \frac{1}{K} \sum_{k=1}^K I\{R(\psi)^k \leq R(\psi)^{obs}\} \quad (5)$$

are uniform on $(0, 1)$ under repeated sampling with error of order $O(n^{-3/2})$ ([Lee and Young, 2005](#)). Similar results hold for $S(\psi)$ and $T(\psi)$ ([Lee and Young, 2005](#); [Young, 2009](#)) with p -values \hat{p}_1^S and \hat{p}_2^S , and \hat{p}_1^T and \hat{p}_2^T , respectively.

The advantage of bootstrap p -values in (4) and (5) over the use of analytical modifications to common statistics is that bootstrap does not require any additional, often tedious, algebraic derivations and implementation of the necessary modifications. Moreover, there are non-standard modelling settings, where $R(\psi)$ is computable while $R^*(\psi)$ is not. One instance is when one or more components of $\hat{\theta}^{obs}$ are on the boundary of the parameter space. The main disadvantage of bootstrap is the additional computation that is typically required for the repeated model fits, which can be partly mitigated by parallel computing.

In some special cases, the distribution of (1), (2) and (3) depends only on ψ , so that constrained bootstrap, as well as simulating data at $(\psi, \hat{\lambda}^\top)^\top$ or even at $(\psi, l^\top)^\top$ for arbitrary nuisance vectors l , produces samples from the hypothesized model. This is the case when the model for fixed ψ is a transformation model (see Severini, 2000, Section 1.3). For instance, if y is a realization of $Y = (Y_1, \dots, Y_n)^\top$ with independent and identically distributed components with generic density

$$g(y_i; \psi, \lambda) = \frac{1}{\lambda} g^0(y_i/\lambda; \psi),$$

we may write $Y_i = \lambda Y_i^0$, with $Y_i^0 \sim g^0(y_i; \psi) = g(y_i; \psi, 1)$. Hence, due to equivariance of the maximum likelihood estimator, $\hat{\lambda}$ and $\lambda \hat{\lambda}^0$ have the same distribution, where $\hat{\lambda}^0$ is the maximum likelihood estimator of λ based on Y_i^0 's. The same representation holds for $\hat{\lambda}_\psi$, so that the profile likelihood ratio

$$\exp\{l(\hat{\psi}, \hat{\lambda}) - l(\psi, \hat{\lambda}_\psi)\} = \prod_{i=1}^n \frac{\hat{\lambda}_\psi g^0(Y_i/\hat{\lambda}; \hat{\psi})}{\hat{\lambda} g^0(Y_i/\hat{\lambda}_\psi; \psi)}$$

has the same distribution as

$$\prod_{i=1}^n \frac{\lambda \hat{\lambda}_\psi^0 g^0\left(\frac{\lambda Y_i^0}{\lambda \hat{\lambda}_\psi^0}; \hat{\psi}\right)}{\lambda \hat{\lambda}_\psi^0 g^0\left(\frac{\lambda Y_i^0}{\lambda \hat{\lambda}_\psi}; \psi\right)} = \prod_{i=1}^n \frac{\hat{\lambda}_\psi^0 g^0(Y_i^0/\hat{\lambda}_\psi^0; \hat{\psi})}{\hat{\lambda}_\psi^0 g^0(Y_i^0/\hat{\lambda}_\psi; \psi)},$$

which depends on ψ only.

3 Two-index asymptotic theory for stratified models

We consider a stratified setting with q independent strata with m observations each. Therefore, the total number of observations is $n = mq$. The models considered here have $\lambda = (\lambda_1, \dots, \lambda_q)^\top$ as nuisance parameter, where λ_i is a stratum-specific parameter. Let $y_i = (y_{i1}, \dots, y_{im})^\top$ ($i = 1, \dots, q$) denote the vector of observations in the i th stratum and let $y = (y_1^\top, \dots, y_q^\top)^\top$. The vectors y_1, \dots, y_q are assumed to be realizations of independent random variables Y_1, \dots, Y_q from a parametric model with densities $g_1(y_1; \psi, \lambda_1), \dots, g_q(y_q; \psi, \lambda_q)$, respectively. The observations within strata are also assumed to be realizations of independent random variables, so that $g_i(y_i; \psi, \lambda_i) = \prod_{j=1}^m g_{ij}(y_{ij}; \psi, \lambda_i)$, where $g_{ij}(\cdot)$ may be conditional on a covariate vector x_{ij} . Under this specification, for fixed ψ , the likelihood has separable parameters $\lambda_1, \dots, \lambda_q$, so that $U_p(\psi) = \sum_{i=1}^q U_\psi^i(\psi, \hat{\lambda}_{i\psi})$, where U_ψ^i is the contribution to U_ψ from the i th stratum.

We work in a two-index asymptotic setting where q increases with m , as $q = O(m^\alpha)$, $\alpha > 0$. The case $\alpha = 0$ corresponds to the standard asymptotic setting. Sartori (2003, Section 4) showed that in the two-index asymptotic setting $R(\psi)$, $S(\psi)$ and $T(\psi)$ are asymptotically equivalent to order $o_p(1)$ for $\alpha \geq 0$.

In the following, we focus on the case when m does not grow faster than q , i.e., $\alpha \geq 1$. In this scenario, $R(\psi)$, $S(\psi)$ and $T(\psi)$ are not asymptotically standard normal, so that, for instance, $\Phi\{R(\psi)\}$ is not asymptotically uniform. Moreover, when $\alpha \geq 1$, the equivalence of the three quantities holds with relative error of order $O_p(m^{-1})$, as opposed to order $O_p(n^{-1/2}) = O_p(m^{-(\alpha+1)/2})$ when $0 < \alpha < 1$ (Sartori, 2003, Section 4).

Theory is more straightforward for $S(\psi)$ than for $R(\psi)$ and $T(\psi)$ because the profile score is the sum of strata profile scores. From Sartori (2003, formula (8)), $S(\psi) = Z + O_p(m^{(\alpha-1)/2})$, where Z is random variable with a standard normal distribution.

Let $F_\theta(\cdot)$ denote the distribution function of $S(\psi)$ under θ , so that $F_\theta(S(\psi))$ is exactly uniform. Lee and Young (2005) proved that, in standard asymptotic settings,

$$\text{pr}_\theta \left(F_{\hat{\theta}_\psi} (S(\psi)) \leq u \right) = u + O(n^{-3/2}) \quad (6)$$

and

$$\text{pr}_\theta (F_{\hat{\theta}}(S(\psi)) \leq u) = u + O(n^{-1}), \quad (7)$$

that is $F_{\hat{\theta}_\psi}(S(\psi))$ and $F_{\hat{\theta}}(S(\psi))$ are asymptotically uniform, with constrained bootstrap being asymptotically more accurate. The same results hold for any pivot asymptotically equivalent to $S(\psi)$ to first-order.

The core result of the current paper is that asymptotic validity of both constrained and unconstrained bootstrap is guaranteed even in a two-index asymptotic setting with $\alpha \geq 1$, provided that $\alpha < 3$, that is $q = o(m^3)$. The latter condition is the same to the one required for validity of inference based on the modified signed likelihood root $R^*(\psi)$ (Sartori, 2003). In particular, we show that

$$\text{pr}_\theta \left(F_{\hat{\theta}_\psi}(S(\psi)) \leq u \right) = u + O(m^{(\alpha-3)/2}). \quad (8)$$

and that

$$\text{pr}_\theta (F_{\hat{\theta}}(S(\psi)) \leq u) = u + O(m^{(\alpha-3)/2}). \quad (9)$$

Hence, the same order of error is obtained both with constrained and unconstrained bootstrap, unlike what happens in standard asymptotic settings.

In order to prove both (8) and (9) we need some preliminary results about the distribution function $F_\theta(x)$ of $S(\psi)$ in the two-index asymptotic setting. From Sartori (2003, formula (6)), $U_p = U_p(\psi)$ can be expanded as

$$U_p = U_{\psi|\lambda} + B + Re, \quad (10)$$

where $U_{\psi|\lambda} = U_\psi - i_{\psi\lambda} i_{\lambda\lambda}^{-1} U_\lambda = O_p(\sqrt{n}) = O_p(m^{(\alpha+1)/2})$, having zero mean and variance $i_{\psi\psi\cdot\lambda}$, $B = B(\theta) = O_p(m^\alpha)$, and, with $\alpha > 1$, $Re = O_p(m^{\alpha-1})$.

Let $M(\theta) = \text{E}_\theta(S(\psi))$ and $\text{Var}_\theta(S(\psi))$ be the expectation and variance of $S(\psi)$. Asymptotic expansions detailed in the Appendix can be used to show that

$$M(\theta) = \frac{b(\theta)}{i_{\psi\psi\cdot\lambda}(\theta)^{1/2}} + M_1(\theta) + O(m^{-(\alpha+1)/2}) \quad (11)$$

$$\text{Var}_\theta(S(\psi)) = 1 + v(\theta) + O(1/m^2), \quad (12)$$

where $b(\theta) = \text{E}_\theta(B) = O(m^\alpha)$, $M_1(\theta) = O(m^{(\alpha-3)/2})$ and $v(\theta) = \text{E}_\theta\{U_{\psi|\lambda}B\}/i_{\psi\psi\cdot\lambda} = O(1/m)$. The cumulants of $S(\psi)$ of order $r \in \{3, 4, \dots\}$ are $O(m^{(\alpha+1)(1-r/2)}) = O(n^{1-r/2})$, as in standard asymptotics.

We assume that the distribution function of $S(\psi)$ admits a valid Edgeworth expansion. In particular, if $S(\psi)$ has a continuous distribution,

$$F_\theta(x) = \text{pr}_\theta (S(\psi) \leq x) = \Phi \left(\frac{x - M(\theta)}{\sqrt{\text{Var}_\theta(S(\psi))}} \right) + O(m^{-(\alpha+1)/2}). \quad (13)$$

Let $x^*(\theta) = (x - M(\theta))/\sqrt{1 + v(\theta)}$. Then

$$\frac{x - M(\theta)}{\sqrt{\text{Var}_\theta(S(\psi))}} = \frac{x - M(\theta)}{\sqrt{1 + v(\theta) + O(1/m^2)}} = x^*(\theta) + O(1/m^2)$$

and

$$F_\theta(x) = \Phi(x^*(\theta)) + O\left(m^{-\min(2, \frac{\alpha+1}{2})}\right). \quad (14)$$

We first focus on constrained bootstrap. From (14),

$$F_{\hat{\theta}_\psi}(x) = \Phi\left(x^*(\hat{\theta}_\psi)\right) + O_p\left(m^{-\min(2, \frac{\alpha+1}{2})}\right). \quad (15)$$

The Taylor expansions in the Appendix give

$$M(\hat{\theta}_\psi) = M(\theta) + \Delta + O_p\left(m^{-\min(1, \frac{5-\alpha}{2})}\right) \quad (16)$$

and

$$v(\hat{\theta}_\psi) = v(\theta) + O_p(m^{-2}), \quad (17)$$

where $\Delta = O_p(m^{(\alpha-3)/2})$ and is given in expression (28) of the Appendix. Using (16) and (17), we can write $x^*(\hat{\theta}_\psi) = x^*(\theta) - \Delta + O_p(m^{-\min(1, (5-\alpha)/2)})$. As a result, provided $\alpha < 3$, the following Taylor expansion of (15) holds

$$F_{\hat{\theta}_\psi}(x) = F_\theta(x) - \phi(x^*(\theta))\Delta + O_p(m^{-1}), \quad (18)$$

where the error is of order $O_p(m^{-1})$ because, with $\alpha < 3$, we have $\min(1, (5-\alpha)/2) = 1$, while the error term in (15) is $o_p(1/m)$ whenever $\alpha > 1$.

In order to prove (8), note that $F_{\hat{\theta}_\psi}(S(\psi)) \leq u$ is equivalent to $S(\psi) \leq s_u$, with s_u the u -quantile of $F_{\hat{\theta}_\psi}(\cdot)$, such that $F_{\hat{\theta}_\psi}(s_u) = u$. Let s_u^0 be the u -quantile of $F_\theta(\cdot)$. It is useful to express s_u in terms of s_u^0 . Using (18),

$$u = F_\theta(s_u^0) = F_{\hat{\theta}_\psi}(s_u) = F_\theta(s_u) - \phi(s_u^*(\theta))\Delta + O_p(m^{-1}),$$

where $s_u^*(\theta) = (s_u - M(\theta))/\sqrt{1+v(\theta)}$. Hence, $F_\theta(s_u) - F_\theta(s_u^0) = \phi(s_u^*(\theta))\Delta + O_p(m^{-1})$. On the other hand, letting $F'_\theta(x) = dF_\theta(x)/dx$, from

$$F_\theta(s_u^0) = F_\theta(s_u) + (s_u^0 - s_u)F'_\theta(s_u) + O_p((s_u^0 - s_u)^2)$$

and

$$F'_\theta(x) = \phi(x^*(\theta))/\sqrt{1+v(\theta)} + O(m^{-(\alpha+1)/2}) = \phi(x^*(\theta)) + O(m^{-1})$$

we get

$$s_u = s_u^0 + \Delta + O_p(m^{-1}) + O_p(m^{\alpha-3}),$$

where the $O_p(m^{\alpha-3})$ term on the right hand side comes from $O_p((s_u^0 - s_u)^2)$. Hence, $S(\psi) \leq s_u$ is equivalent to $S(\psi) \leq s_u^0 + \Delta + O_p(m^{-1}) + O_p(m^{\alpha-3})$, and

$$\text{pr}_\theta\left(F_{\hat{\theta}_\psi}(S(\psi)) \leq u\right) = \text{pr}_\theta\left(\bar{S}(\psi) \leq F_\theta^{-1}(u)\right),$$

where $\bar{S}(\psi) = S(\psi) - \Delta + O_p(m^{\alpha-3}) + O_p(m^{-1})$, with Δ given by (28), and such that $E_\theta(\Delta) = O(m^{(\alpha-3)/2})$. Moreover, we have

$$E_\theta(\bar{S}(\psi)) = E_\theta(S(\psi)) + O(m^{(\alpha-3)/2}), \quad (19)$$

$$\text{Var}_\theta(\bar{S}(\psi)) = \text{Var}_\theta(S(\psi)) + O(1/m^2), \quad (20)$$

so that (8) holds because

$$\text{pr}_\theta\left(\bar{S}(\psi) \leq F_\theta^{-1}(u)\right) = \text{pr}_\theta\left(S(\psi) \leq F_\theta^{-1}(u)\right) + O(m^{(\alpha-3)/2}) = u + O(m^{(\alpha-3)/2}).$$

The proof of (9) for unconstrained bootstrap is obtained along the same steps as above. Details are provided in the Appendix. The key observation for that proof is that an expansion for $F_{\hat{\theta}}(x)$ of the form (18) holds with a different Δ term, which is still of order $O_p(m^{(\alpha-3)/2})$.

Table 1: Statistics considered for the results of the simulation experiments. The mean $\tilde{\mu}_R$ and the standard deviation $\tilde{\sigma}^R$ of $R(\psi)$ are estimated through constrained bootstrap, by simulating from the model at $\theta = \hat{\theta}_\psi$.

Statistic	Plotting Symbol	Description
$R(\psi)$	R	Signed likelihood root
$R^*(\psi)$	R^*	Modified signed likelihood root
$\Phi^{-1}\{\hat{p}^R(\psi)\}$	R^u	Transformed p -value from unconstrained bootstrap of $R(\psi)$
$\Phi^{-1}\{\hat{p}_2^R(\psi)\}$	R^c	Transformed p -value from constrained bootstrap of $R(\psi)$
$R(\psi) - \tilde{\mu}^R$	R_l^c	Location adjusted $R(\psi)$
$(R(\psi) - \tilde{\mu}^R)/\tilde{\sigma}^R$	R_{ls}^c	Location-and-scale adjusted $R(\psi)$

4 Simulation studies

The finite-sample properties of unconstrained and constrained parametric bootstrap are assessed through extensive simulation studies, for four statistical models for stratified data. In particular, we consider a gamma model, a beta model, a curved exponential family model and a multi-sample Behrens-Fisher setting. For each model, we conduct 9 simulation experiments, one for each combination of number of strata $q \in \{10, 100, 1000\}$ and stratum sample size $m \in \{4, 8, 16\}$.

Each simulation experiment involves 10000 simulated samples under the model at a fixed parameter vector $\theta_0 = (\psi_0, \lambda_0^\top)^\top$. For each simulated sample, 17 statistics and 6 bootstrap-based p -values are computed for testing $\psi = \psi_0$. In particular, the statistics that are computed are i) $R(\psi)$, $S(\psi)$, $T(\psi)$, ii) the location and location-and-scale adjusted versions of $R(\psi)$, $S(\psi)$, $T(\psi)$, where the mean and variance of each statistic are estimated using unconstrained bootstrap (at $\hat{\theta}$) and constrained bootstrap (at $\hat{\theta}_\psi$), and iii) $R^*(\psi)$ and the signed likelihood root computed from the modified profile likelihood (see, for instance Severini, 2000, Chapter 8). The higher-order adjustment required for the latter two statistics is obtained using expected moments of likelihood quantities as in Severini (2000, §7.5). Finally, for each of $R(\psi)$, $S(\psi)$, and $T(\psi)$, we compute the unconstrained and constrained bootstrap p -values in (4) and in (5), respectively.

In the interest of space, in what follows, we only report results for the 6 statistics based on $R(\psi)$ shown in Table 1. The conclusions for the remaining statistics and p -values are qualitatively the same. Results are also only presented for $(q, m) = (10, 4)$, $(q, m) = (100, 4)$, $(q, m) = (1000, 4)$, $(q, m) = (1000, 8)$, and $(q, m) = (1000, 16)$, because these combinations of q and m are sufficient for assessing the performance of the statistics as q and m grow. The results from all simulation experiments are provided in the Supplementary Material.

The above experiments involve high-dimensional parameter spaces with as many as 1000 nuisance parameters. As a result, the assessment of the statistics requiring bootstrapping is demanding in terms of computational time and cost, even when parallel computing with a large number of cores is used. For this reason, the number of bootstrap samples is limited to 1000 in all simulation experiments.

The 4 blocks of rows in Table 2 give the estimated tail probabilities of the statistics of interest for the case $q = 1000$ and $m = 8$ for all four models considered. This combination of q and m was selected because it is the least extreme setting (compared to the most extreme $q = 1000$, $m = 4$) where departures from the expected behaviour in terms of the distribution of the statistics start becoming apparent; the results for all the other combinations of q and m are provided in the Supplementary Material. The following sections give a more detailed discussion

on the figures shown in Table 2.

Table 2: Empirical tail probabilities $\times 100$ for the statistics in Table 1 and all models considered in the simulation studies of Section 4. The figures shown have been rounded to 1 decimal and are for $q = 1000$ and $m = 8$.

Model	Statistic	Nominal					
		1.0	2.5	5.0	95.0	97.5	99.0
Gamma	R	0.0	0.0	0.0	0.0	0.0	0.0
	R^*	0.7	1.5	3.3	92.1	95.5	98.2
	R^u	1.1	2.7	5.3	95.1	97.7	99.2
	R^c	1.0	2.5	5.0	94.6	97.2	99.0
	R_l^c	1.1	2.8	5.4	94.2	96.8	98.9
	R_{ls}^c	1.1	2.5	4.9	94.5	97.2	99.1
Beta	R	0.0	0.0	0.0	0.0	0.0	0.0
	R^*	0.7	1.8	3.8	93.7	96.8	98.8
	R^u	0.8	1.9	4.1	94.0	97.0	98.7
	R^c	1.0	2.3	4.8	95.0	97.4	99.1
	R_l^c	1.1	2.5	5.1	94.7	97.3	98.9
	R_{ls}^c	0.9	2.3	4.8	95.1	97.5	99.0
Curved exponential family	R	100.0	100.0	100.0	100.0	100.0	100.0
	R^*	1.4	3.5	6.9	96.6	98.3	99.4
	R^u	0.6	1.8	4.0	95.0	97.7	99.2
	R^c	1.2	3.3	6.4	96.2	98.2	99.4
	R_l^c	1.5	3.6	7.1	95.8	98.0	99.2
	R_{ls}^c	1.3	3.2	6.5	96.3	98.2	99.4
Behrens-Fisher	R	2.4	4.6	7.6	92.1	95.6	98.0
	R^*	1.2	2.8	5.3	94.8	97.5	99.0
	R^u	1.1	2.7	5.2	95.0	97.6	99.1
	R^c	1.1	2.7	5.1	94.9	97.6	99.1
	R_l^c	2.4	4.7	7.6	92.1	95.5	98.0
	R_{ls}^c	1.1	2.6	5.1	95.0	97.6	99.1

4.1 Gamma model

As a first example we take a stratified gamma model with common shape parameter, for which Y_{ij} has density function

$$g(y_{ij}; \alpha, \beta_i) = \frac{1}{\Gamma(\alpha) \beta_i^\alpha} y_{ij}^{\alpha-1} \exp\left\{-\frac{y_{ij}}{\beta_i}\right\} \quad (y_{ij} > 0),$$

where $\Gamma(\cdot)$ is the gamma function. The parameter of interest is $\psi = \log(\alpha)$ and the stratum-specific nuisance parameters are given by $\lambda_i = \log(\beta_i)$. The simulation data sets were generated for $\psi_0 = \log(2)$ and the elements of λ_0 are fixed to the logarithm of random draws from an exponential distribution with rate 1/2.

The left panel of Figure 1 shows the empirical densities for the statistics in Table 1. The performance of the statistics is evaluated in terms of the closeness of their empirical density to

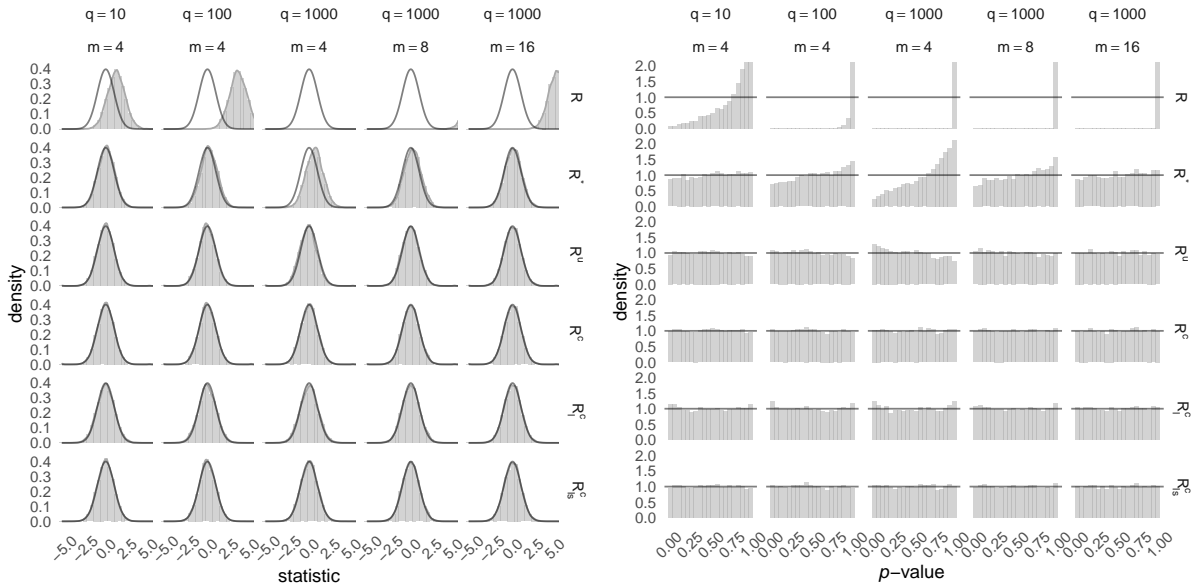


Figure 1: Gamma model. Estimated null distribution of statistics (left) and estimated distribution of p -values (right) for the statistics in Table 1 for various combinations of q and m . The $N(0, 1)$ and $\text{Uniform}(0, 1)$ density functions are superimposed for statistics (left) and p -values (right).

the standard normal density. This assessment is valid also for the constrained and unconstrained bootstrap p -values, since they have been mapped into the standard normal scale by the $\Phi^{-1}(\cdot)$ transformation.

The large location bias of the distribution of $R(\psi)$ is apparent for all shown combinations of q and m , and it becomes huge for $q = 1000$ and $m \in \{4, 8\}$. All higher-order accurate statistics result in a marked finite-sample correction, with $R^*(\psi)$ and the unconstrained bootstrap illustrating some discrepancy from the standard normal distribution, especially for $(q, m) = (1000, 4)$. This is more noticeable for $R^*(\psi)$, and it is also apparent from the entries in Table 2. On the other hand, results in Figures S1-S2 in the Supplementary Material show that the signed likelihood root computed from the modified profile likelihood is more accurate than R^* in the most extreme settings.

From the right panel of Figure 1, it is apparent that the p -values based on R^c , the location adjusted version R_l^c and the location-and-scale adjusted version R_{ls}^c are all close to one another. Hence, the necessary adjustment for making the distribution of $R(\psi)$ to be close to standard normal is mainly a location adjustment.

Note that the Gamma model we use here is a transformation model. Then, as shown at the end of Section 2, constrained bootstrap produces Monte Carlo samples from the hypothesized distribution, which is not necessarily true for unconstrained bootstrap. As a result, the better performance of the former for large q/m ratios is not surprising.

4.2 Beta model

Suppose that Y_{ij} has a beta distribution, with density function

$$g(y_{ij}; \mu_i, \phi) = \frac{1}{B\{\mu_i\phi, (1 - \mu_i)\phi\}} y_{ij}^{\mu_i\phi - 1} (1 - y_{ij})^{(1 - \mu_i)\phi - 1} \quad (0 < y_{ij} < 1),$$

where $B(\cdot)$ is the beta function. The parameter of interest is $\psi = \log \phi$, whereas the stratum-specific nuisance parameters are given by $\lambda_i = \log\{\mu_i/(1 - \mu_i)\}$. The simulation experiments

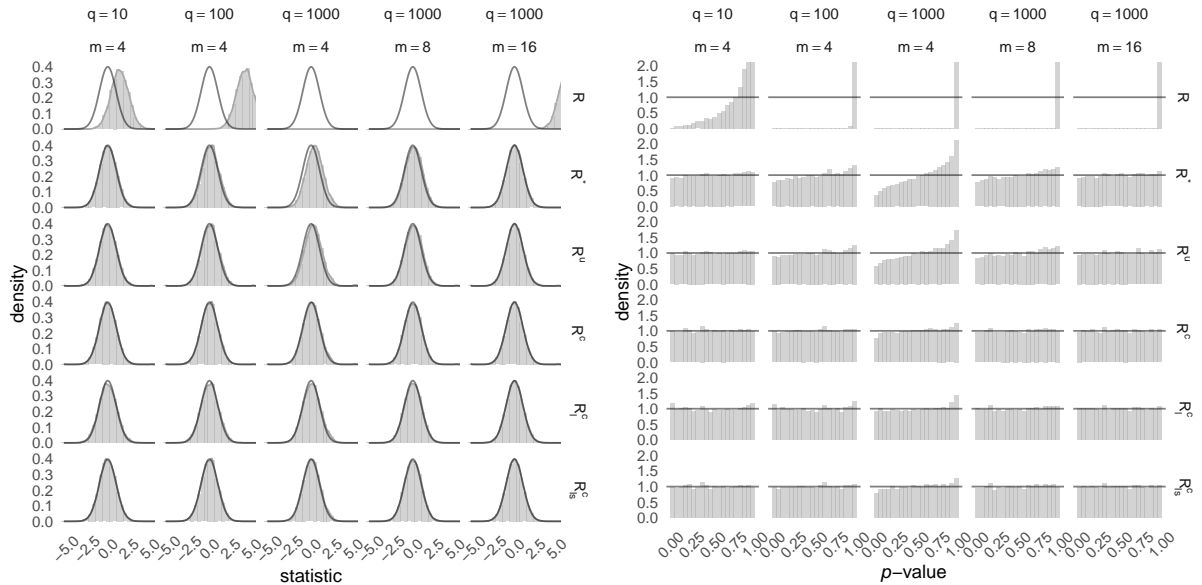


Figure 2: Beta model. Estimated null distribution of statistics (left) and estimated distribution of p -values (right) for the statistics in Table 1 for various combinations of q and m . The $N(0, 1)$ and $Uniform(0, 1)$ density functions are superimposed for statistics (left) and p -values (right).

are carried out for $\psi_0 = \log(2)$ and the elements of λ_0 are generated from a standard normal distribution.

The results summarised in Figure 2 are similar to those of the gamma example. Both constrained and unconstrained bootstrap deliver marked corrections to the distribution of R . As is also apparent in Table 2, the finite-sample distributions of the constrained bootstrap p -values are closer to uniform than those coming from unconstrained bootstrap for large q/m ratios, such as $q = 1000$ and $m \in \{4, 8\}$.

4.3 Curved exponential family

This example involves normally distributed random variables Y_{ij} , each with mean $\exp(\lambda_i)$ and variance $\exp(\psi + \lambda_i/2)$. This model was studied in Sartori et al. (1999), where it is pointed out that a marginal likelihood for ψ is not available. The simulation experiments are carried out for $\psi_0 = \log(1/2)$ and the elements of λ_0 are generated from a standard normal distribution.

The left panel in Figure 3 shows the empirical density functions of the statistics in Table 1, and the right panel shows the corresponding p -value distributions. Again, the empirical, finite-sample distributions of $R(\psi)$ are far from standard normal, while all the higher-order statistics perform considerably better. The conclusions are similar to those from the simulation experiments for the gamma and beta models, in that the required adjustment to $R(\psi)$ seems to be a location correction. The main difference is the fact that no statistic appears to perform well for $(q, m) = (1000, 4)$; see, also the empirical tail probabilities in Table 2.

4.4 Behrens-Fisher model

Suppose that Y_{ij} are normally distributed, with common mean ψ across all strata, and stratum-specific variances $\exp(\lambda_i)$. This example was studied in Young (2009), where it is illustrated that $R^*(\psi)$ is performing worse than constrained bootstrapping of $R(\psi)$ in a simulation study with $q = 20$ strata and the stratum sample size varying between 3 and 10. The simulation experiments are carried out for $\psi_0 = 0$ and λ_0 generated from a uniform distribution in $(0, 1)$.

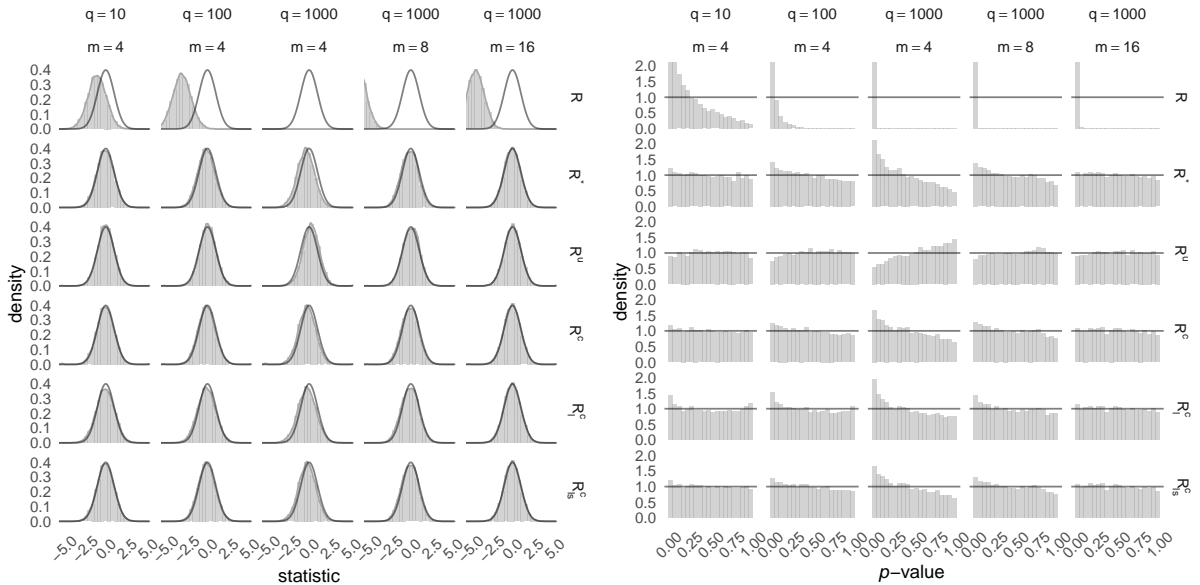


Figure 3: Curved exponential family model. Estimated null distribution of statistics (left) and estimated distribution of p -values (right) for the statistics in Table 1 for various combinations of q and m . The $N(0, 1)$ and $\text{Uniform}(0, 1)$ density functions are superimposed for statistics (left) and p -values (right).

The findings in Young (2009) are confirmed also in the more extensive simulation studies here, whose results are reported in Figure 4. For the Behrens-Fisher model, the location-adjustment to $R(\psi)$ does not have much of an effect to the distribution of the statistic. On the other hand, the location-and-scale adjusted statistic recovers inferential performance. So, it seems that only a scale adjustment is sufficient to recover first-order inferential performance; see also Table 2. Indeed, for this model the profile score bias is exactly equal to zero, so that the distribution of the first-order statistic $R(\psi)$ is essentially centred around zero. Also, both constrained and unconstrained bootstrap perform extremely well across all the simulation scenarios, and, along with R_{ls}^c , they outperform $R^*(\psi)$ in the most extreme settings.

A remarkable observation in this model is the excellent accuracy of the score statistic $S(\psi)$ for all combination of q and m considered (see the Supplementary Material for the full results). This can be explained by the fact that the leading term $U_{\psi|\lambda}$ of U_p in (10) is exactly normally distributed. Moreover, $M(\theta)$ and $v(\theta)$, in (11) and (12) respectively, are equal to zero.

5 Concluding remarks

The contribution of this paper is to formally show that, in stratified settings, inference based on either unconstrained or constrained parametric bootstrap of usual likelihood pivots is effective in recovering their inferential performance, even in rather extreme settings, where the bias of the profile score prevents valid first-order inference.

Unconstrained and constrained bootstrap for the signed likelihood ratio root, the score statistic and the Wald statistic can both recover inferential performance in stratified settings when $q = O(m^\alpha)$, for $0 < \alpha < 3$. This is different from the standard asymptotic setting when $\alpha = 0$, where constrained bootstrap asymptotically outperforms unconstrained bootstrap (Lee and Young, 2005). The condition $q = O(m^\alpha)$, for $0 < \alpha < 3$, is the same as the one found in Sartori (2003) for validity of inference based on R^* and on the signed likelihood root computed from the modified profile likelihood.

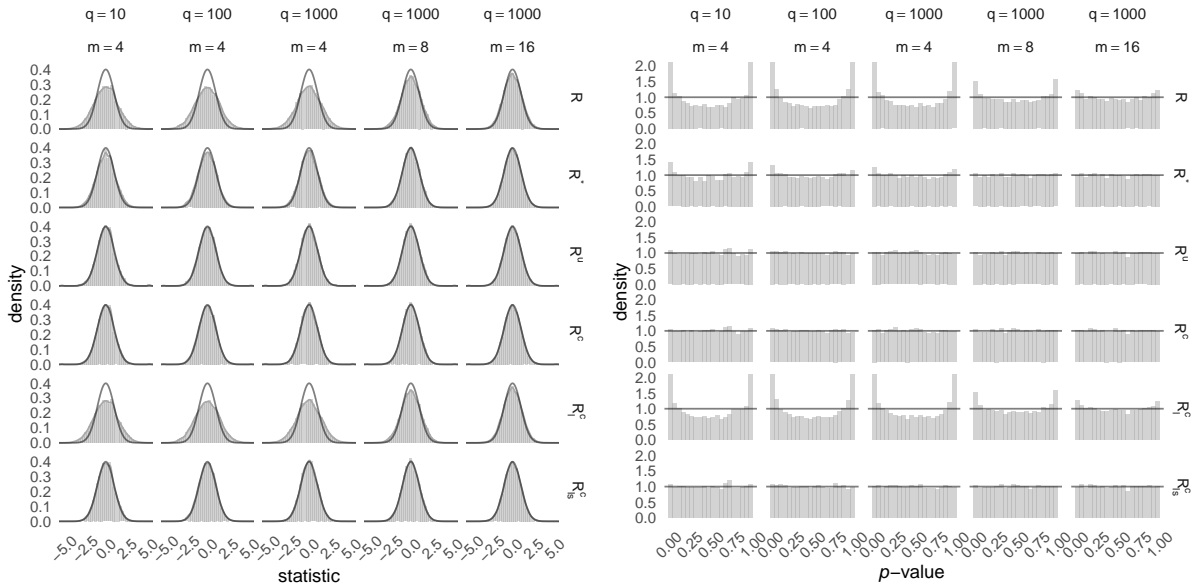


Figure 4: Behrens-Fisher model. Estimated null distribution of statistics (left) and estimated distribution of p -values (right) for the statistics in Table 1 for various combinations of q and m . The $N(0, 1)$ and $\text{Uniform}(0, 1)$ density functions are superimposed for statistics (left) and p -values (right).

The results of Section 4 from the extensive simulation studies for the finite-sample assessment of the performance of constrained and unconstrained bootstrap are in par to what is expected from theory. In extreme settings, like the Beta model with $(q, m) = (1000, 4)$, constrained bootstrap appears to perform slightly better than unconstrained bootstrap. Furthermore, in all simulation experiments we carried out and as q/m diverges, the inferential performance from constrained and unconstrained bootstrap of first-order statistics seems to be deteriorating much slower than that of R^* and the signed likelihood root computed from the modified profile likelihood (see also the Supplementary Material). As a result, the evidence from the simulation studies points out that inference from parametric bootstrap is more resilient to increasing q/m than inference from well-used, analytically available higher-order statistics.

The theoretical developments in this paper do not immediately cover situations where the random variables have discrete support, because the Edgeworth expansion in (13) is only valid for models with continuous support. The impact of discreteness on the performance of parametric bootstrap is examined in the Supplementary Material through a binomial matched pairs model. In particular, the experimental setup of Section 4 is used for a stratified logistic regression model, where Y_{ij} has a Bernoulli distribution with probability $\exp(\lambda_i + \psi x_j) / \{1 + \exp(\lambda_i + \psi x_j)\}$, with $x_j = 1$ for $j \in \{1, \dots, m/2\}$ and $x_j = 0$ for $j \in \{m/2 + 1, \dots, m\}$. The results in Figures S17-S20 and Tables S3-S11 in the Supplementary Material indicate that the equivalence between unconstrained and constrained bootstrap of the first-order statistics in continuous models may not hold for discrete settings. Despite that unconstrained bootstrap delivers a marked inferential improvement to first-order statistics, constrained bootstrap, similarly to R^* , is found to perform considerably better for most combinations of q and m .

The simulation experiments in this paper have been carried out with 1000 bootstrap replications. This value is smaller than some of the recommendations of millions of replications that have appeared in the literature for standard asymptotics settings (Young, 2009; DiCiccio et al., 2017). For stratified settings with $\alpha > 1$ the bootstrap adjustments have the role of recovering asymptotic uniformity of p -values, rather than providing a small-sample refinement of p -values

that are asymptotically uniform. As a result, use of a huge number of bootstrap replications is less essential. Some limited experiments with more than 1000 bootstrap replications seem to point in this direction. More comprehensive simulation experiments to confirm that statement are unfortunately not feasible with current computing capabilities.

Acknowledgements

Ioannis Kosmidis is supported by The Alan Turing Institute under the EPSRC grant EP/N510129/1. Part of this work was completed during a visit of Ruggero Bellio, Alessandra Salvan and Nicola Sartori to The Alan Turing Institute. Alessandra Salvan and Nicola Sartori have been supported by the University of Padova under grant BIRD185955.

Supplementary Material

The Supplementary Material provides the outputs from the simulation experiments described in Section 4, for all models and all combinations of statistics, q and m . Outputs are also provided for the logistic regression model described in Section 5. The outputs include null distributions of the various statistics and distributions of p -values, through extended versions of the Figures 1-4, and empirical tail probabilities, through extended versions of Table 2.

Appendix

Derivation of (11) and (12)

The following representation from Sartori (2003, Appendix) will be used to determine the order of quantities in a stratified setting. Let μ_i and σ_i^2 to denote mean and variance of independent the random variables X_1, \dots, X_q . Then

$$\sum_{i=1}^q X_i = O_p\left(\sum_{i=1}^q \mu_i\right) + O_p\left(\sqrt{\sum_{i=1}^q \sigma_i^2}\right). \quad (21)$$

We have $U_\psi = \sum_{i=1}^q U_\psi^i$, where U_ψ^i is the contribution to U_ψ from the i th stratum, and $U_\lambda = (U_{\lambda_1}, \dots, U_{\lambda_q})^\top$. Here and in the following, when the argument is omitted, evaluation at θ is understood.

The terms on the right-hand side of (10) are seen to be of order $O_p(m^{(\alpha+1)/2})$, $O_p(m^\alpha)$ and $O_p(m^{\alpha-1})$, respectively. Indeed, using (21), we have $U_{\psi|\lambda} = \sum_{i=1}^q U_{\psi|\lambda_i} = O_p(m^{(\alpha+1)/2})$, with $U_{\psi|\lambda_i} = U_\psi^i - i_{\psi\lambda_i} i_{\lambda_i\lambda_i}^{-1} U_{\lambda_i}$ being $E_\theta(U_{\psi|\lambda_i}) = 0$ and $\text{Var}_\theta(U_{\psi|\lambda_i}) = i_{\psi\psi\cdot\lambda_i} = O(m)$. Note that $i_{\psi\psi\cdot\lambda} = \text{Var}_\theta(U_{\psi|\lambda}) = \sum_{i=1}^q i_{\psi\psi\cdot\lambda_i}$. Similarly, we have $B = \sum_{i=1}^q B^i(\psi, \lambda_i) = O_p(m^\alpha)$, where $B^i(\psi, \lambda_i)$ is the term of order $O_p(1)$ of the expansion of the profile score in the i th stratum, having both mean and variance of order $O(1)$. The same additivity property holds for $b(\theta)$, so that $b(\theta) = \sum_{i=1}^q b^i(\psi, \lambda_i) = O(m^\alpha)$. Finally, the remainder term is $Re = \sum_{i=1}^q Re^i(\psi, \lambda_i)$, with $Re^i(\psi, \lambda_i)$ having mean and variance of order $O(1/m)$, so that $Re = O_p(m^{\max\{\alpha-1, (\alpha-1)/2\}}) = O_p(m^{\alpha-1})$ when $\alpha > 1$.

Moreover, we have

$$i_{\psi\psi\cdot\lambda}(\hat{\theta}_\psi) = i_{\psi\psi\cdot\lambda} + C + O_p(m^{\alpha-1}), \quad (22)$$

where

$$C = \sum_{i=1}^q \frac{d}{d\lambda_i} i_{\psi\psi\cdot\lambda_i}(\hat{\lambda}_{i\psi} - \lambda_i) + \frac{1}{2} \sum_{i=1}^q \frac{d^2}{d\lambda_i^2} i_{\psi\psi\cdot\lambda_i}(\hat{\lambda}_{i\psi} - \lambda_i)^2 = O_p(m^\alpha),$$

where the order is again determined using (21). Hence,

$$\{i_{\psi\psi\cdot\lambda}(\hat{\theta}_\psi)\}^{-1/2} = i_{\psi\psi\cdot\lambda}^{-1/2} \left\{ 1 - \frac{1}{2} \frac{C}{i_{\psi\psi\cdot\lambda}} + O_p(m^{-2}) \right\}, \quad (23)$$

with $C/i_{\psi\psi\cdot\lambda} = O_p(m^{-1})$.

Using (10) and (23),

$$\begin{aligned} S(\psi) &= i_{\psi\psi\cdot\lambda}^{-1/2} \{U_{\psi|\lambda} + B + Re\} \left\{ 1 - \frac{1}{2} \frac{C}{i_{\psi\psi\cdot\lambda}} + O_p(m^{-2}) \right\} \\ &= \frac{U_{\psi|\lambda}}{i_{\psi\psi\cdot\lambda}^{.1/2}} + \frac{B}{i_{\psi\psi\cdot\lambda}^{.1/2}} + \frac{Re}{i_{\psi\psi\cdot\lambda}^{.1/2}} - \frac{1}{2} \frac{U_{\psi|\lambda}C}{i_{\psi\psi\cdot\lambda}^{.3/2}} - \frac{1}{2} \frac{BC}{i_{\psi\psi\cdot\lambda}^{.3/2}} - \frac{1}{2} \frac{ReC}{i_{\psi\psi\cdot\lambda}^{.3/2}} \\ &\quad + O_p(m^{-2}) + O_p(m^{(\alpha-5)/2}) + O_p(m^{(\alpha-7)/2}), \end{aligned} \quad (24)$$

where $O_p(m^{-2}) + O_p(m^{(\alpha-5)/2}) + O_p(m^{(\alpha-7)/2}) = O_p(m^{(\alpha-5)/2})$ as long as $\alpha > 1$. The term of order $O_p(m^{(\alpha-5)/2})$ is given by $i_{\psi\psi\cdot\lambda}^{-3/2} B$ times the term of order $O_p(m^{-2})$ in (23). Its expectation is of order $O(m^{-(\alpha+5)/2})$. The orders of terms in (24) are as follows:

$$\begin{aligned} \frac{U_{\psi|\lambda}}{i_{\psi\psi\cdot\lambda}^{.1/2}} &= O_p(1), \quad \frac{B}{i_{\psi\psi\cdot\lambda}^{.1/2}} = O_p(m^{(\alpha-1)/2}), \quad \frac{Re}{i_{\psi\psi\cdot\lambda}^{.1/2}} = O_p(m^{(\alpha-3)/2}), \\ \frac{1}{2} \frac{U_{\psi|\lambda}C}{i_{\psi\psi\cdot\lambda}^{.3/2}} &= O_p(1/m) = o_p(1), \quad \frac{1}{2} \frac{BC}{i_{\psi\psi\cdot\lambda}^{.3/2}} = O_p(m^{(\alpha-3)/2}), \quad -\frac{1}{2} \frac{ReC}{i_{\psi\psi\cdot\lambda}^{.3/2}} = O_p(m^{\alpha-3}). \end{aligned}$$

Expansion (11) for $E_\theta(S(\psi))$ is obtained using (24) and recalling that $b(\theta) = O(m^\alpha)$. We have

$$\begin{aligned} E_\theta \left(\frac{U_{\psi|\lambda}}{i_{\psi\psi\cdot\lambda}^{.1/2}} \right) &= 0, \quad E_\theta \left(\frac{B}{i_{\psi\psi\cdot\lambda}^{.1/2}} \right) = \frac{b(\theta)}{i_{\psi\psi\cdot\lambda}^{.1/2}} = O(m^{(\alpha-1)/2}), \\ E_\theta \left(\frac{Re}{i_{\psi\psi\cdot\lambda}^{.1/2}} \right) &= O(m^{(\alpha-3)/2}), \quad E_\theta \left(\frac{1}{2} \frac{U_{\psi|\lambda}C}{i_{\psi\psi\cdot\lambda}^{.3/2}} \right) = O(m^{-(\alpha+3)/2}) = o(1), \\ E_\theta \left(\frac{1}{2} \frac{BC}{i_{\psi\psi\cdot\lambda}^{.3/2}} \right) &= O(m^{-(\alpha+1)/2}) = o(1), \quad E_\theta \left(-\frac{1}{2} \frac{ReC}{i_{\psi\psi\cdot\lambda}^{.3/2}} \right) = O(m^{(\alpha-3)/2}), \end{aligned}$$

giving (11) with

$$M_1(\theta) = E_\theta \left(\frac{Re}{i_{\psi\psi\cdot\lambda}^{.1/2}} \right) + E_\theta \left(-\frac{1}{2} \frac{ReC}{i_{\psi\psi\cdot\lambda}^{.3/2}} \right) = O(m^{(\alpha-3)/2}). \quad (25)$$

Expansion (12) for $\text{Var}_\theta(S(\psi))$ is also obtained using (24). In particular, the leading term has variance equal to 1, and, using a standard expansion for the stratum profile score $U_\psi^i(\psi, \hat{\lambda}_{i\psi})$ (see e.g Pace and Salvani, 1997, formula (8.88)), $\text{Cov}_\theta(U_{\psi|\lambda}, B)$ and $\text{Var}_\theta(B)$ are easily seen to be of order $O(m^\alpha)$ and $O(m^{\alpha-1})$, respectively. Further terms of (24) give contributions to the variance of order $o(m^{-2})$.

Higher order cumulants of $S(\psi)$, $r = 3, 4, \dots$, have the form

$$\kappa_r(S(\psi)) = \frac{O(m^{\alpha+1})}{O(m^{r(\alpha+1)/2})} = O(m^{(\alpha+1)(1-r/2)}) = O(n^{1-r/2})$$

as in standard asymptotics.

Derivation of (16) and (17)

Let $\overline{Re} = E_\theta(Re)$. Then, from (11) and (25),

$$M(\hat{\theta}_\psi) = \left\{ i_{\psi\psi\cdot\lambda}(\hat{\theta}_\psi) \right\}^{-1/2} \left\{ b(\hat{\theta}_\psi) + \overline{Re}(\hat{\theta}_\psi) - \frac{1}{2} \frac{1}{i_{\psi\psi\cdot\lambda}(\hat{\theta}_\psi)} E_\theta(Re C) \right\} + O_p(m^{-(\alpha+1)/2}),$$

where $i_{\psi\psi\cdot\lambda}(\hat{\theta}_\psi)^{-1} E_\theta(Re C)$ is seen to be of order $O_p(m^{-1})$. Therefore,

$$M(\hat{\theta}_\psi) = \left\{ i_{\psi\psi\cdot\lambda}(\hat{\theta}_\psi) \right\}^{-1/2} \left\{ b(\hat{\theta}_\psi) + \overline{Re}(\hat{\theta}_\psi) \right\} + O_p(m^{-(\alpha+1)/2}).$$

Now,

$$b(\hat{\theta}_\psi) = b(\theta) + b_1(\theta) + O_p(m^{\alpha-2}), \quad (26)$$

where

$$b_1(\theta) = \sum_{i=1}^q b_{\lambda_i}^i(\psi, \lambda_i) (\hat{\lambda}_{i\psi} - \lambda_i) + \frac{1}{2} \sum_{i=1}^q b_{\lambda_i \lambda_i}^i(\psi, \lambda_i) (\hat{\lambda}_{i\psi} - \lambda_i)^2,$$

and $b_{\lambda_i}^i(\psi, \lambda_i) = \partial b^i(\psi, \lambda_i) / \partial \lambda_i$, and so on. Using (21), and being $b_{\lambda_i}^i(\psi, \lambda_i)$ and $b_{\lambda_i \lambda_i}^i(\psi, \lambda_i)$ both of order $O(1)$,

$$\sum_{i=1}^q b_{\lambda_i}^i(\psi, \lambda_i) (\hat{\lambda}_{i\psi} - \lambda_i) = O_p(m^{\alpha-1}) + O(m^{(\alpha-1)/2})$$

and

$$\sum_{i=1}^q b_{\lambda_i \lambda_i}^i(\psi, \lambda_i) (\hat{\lambda}_{i\psi} - \lambda_i)^2 = O_p(m^{\alpha-1}) + O_p(m^{(\alpha-2)/2}).$$

The remainder in (26) is of order $O_p(m^{\alpha-2}) + O_p(m^{(\alpha-3)/2}) = O_p(m^{\alpha-2})$, when $\alpha > 1$. Moreover, $\overline{Re}(\hat{\theta}_\psi) = \overline{Re} + O_p(m^{(\alpha-1)/2})$.

Using (23), we get

$$M(\hat{\theta}_\psi) = i_{\psi\psi\cdot\lambda}^{-1/2} b(\theta) + \tilde{M}_1 + O_p\left(m^{-\min\{1, (5-\alpha)/2\}}\right), \quad (27)$$

with

$$\tilde{M}_1 = i_{\psi\psi\cdot\lambda}^{-1/2} \left\{ b_1(\theta) - (1/2) C b(\theta) / i_{\psi\psi\cdot\lambda} + \overline{Re} \right\},$$

which is of order $O_p(m^{(\alpha-3)/2})$ because all terms are of the same order.

Therefore, (27) and (24) give (16) with

$$\Delta = \tilde{M}_1 - M_1(\theta) = \frac{b_1(\theta)}{i_{\psi\psi\cdot\lambda}^{-1/2}} - \frac{C b(\theta)}{2 i_{\psi\psi\cdot\lambda}^{3/2}} + \frac{E_\theta(Re C)}{2 i_{\psi\psi\cdot\lambda}^{3/2}} \quad (28)$$

that is of order $O_p(m^{(\alpha-3)/2})$.

To obtain expansion (17) we note that

$$v(\theta) = \frac{1}{i_{\psi\psi\cdot\lambda}} \sum_{i=1}^q v^i(\psi, \lambda_i),$$

where $v^i(\psi, \lambda_i)$ is the $O(1)$ term of $Var_\theta(U_\psi^i(\psi, \hat{\lambda}_{i\psi}))$. From (22),

$$\frac{1}{i_{\psi\psi\cdot\lambda}(\hat{\theta}_\psi)} = \frac{1}{i_{\psi\psi\cdot\lambda}} \left\{ 1 + O(m^{-1}) \right\}. \quad (29)$$

In addition,

$$\begin{aligned}\sum_{i=1}^q v^i(\psi, \hat{\lambda}_{i\psi}) &= \sum_{i=1}^q v^i(\psi, \lambda_i) + \sum_{i=1}^q \frac{d}{d\lambda_i} v^i(\psi, \lambda_i) (\hat{\lambda}_{i\psi} - \lambda_i) + O_p(m^{\alpha-2}) \\ &= \sum_{i=1}^q v^i(\psi, \lambda_i) + O_p(m^{\alpha-1}),\end{aligned}$$

which, combined with (29), gives (17).

Derivation of (9)

First, from (14), we have

$$F_{\hat{\theta}}(x) = \Phi\left(x^*(\hat{\theta})\right) + O_p\left(m^{-\min(2, \frac{\alpha+1}{2})}\right).$$

In order to obtain expansions of $M(\hat{\theta})$ and $v(\hat{\theta})$ around θ , we use the fact that, when $\alpha > 1$, $\hat{\psi} - \psi = O_p(m^{-1})$ (Sartori, 2003). This implies that an expansion for $F_{\hat{\theta}}(x)$ of the form (18) holds with a different Δ term, which is still of order $O_p(m^{(\alpha-3)/2})$ and involves a linear term in $\hat{\theta} - \theta$ and a quadratic term in $\hat{\lambda} - \lambda$. As a consequence, the mean and variance of the analogue of the quantity $\bar{S}(\psi)$ still satisfy (19) and (20). This explains why the order of errors in (8) and (9) is the same, unlike what happens in standard asymptotic settings, where constrained bootstrap formally improves over unconstrained bootstrap, as indicated by (6) and (7).

In order to obtain an expansion for $M(\hat{\theta})$ we follow the same steps as in (26)–(28), giving (16). In particular, we have

$$b(\hat{\theta}) = b(\theta) + b_2(\theta) + O_p(m^{\alpha-2})$$

where

$$\begin{aligned}b_2(\theta) = b_2(\psi, \lambda) &= \sum_{i=1}^q b_{\psi}^i(\hat{\psi} - \psi) + \sum_{i=1}^q b_{\lambda_i}^i(\hat{\lambda}_i - \lambda_i) + \frac{1}{2} \sum_{i=1}^q b_{\lambda_i \lambda_i}^i(\hat{\lambda}_i - \lambda_i)^2 \\ &\quad + \frac{1}{2} \sum_{i=1}^q b_{\psi\psi}^i(\hat{\psi} - \psi)^2 + \sum_{i=1}^q b_{\psi\lambda_i}^i(\hat{\lambda}_i - \lambda_i)(\hat{\psi} - \psi).\end{aligned}\tag{30}$$

From Sartori (2003, below formula (9)), with $\alpha > 1$, $\hat{\psi} - \psi = O_p(m^{-1})$, so that the first three summands on the right hand side of the last formula are of order $O_p(m^{\alpha-1})$, while the remaining two are of order $O_p(m^{\alpha-2})$. This leads to

$$M(\hat{\theta}) = M(\theta) + \Delta_1 + O_p\left(m^{-\min(1, \frac{5-\alpha}{2})}\right)\tag{31}$$

where the term Δ_1 is of order $O_p(m^{(\alpha-3)/2})$, as its expected value, because the leading terms in (30) are of the same order as $b_1(\theta)$ in (26).

Using (31) and an expansion similar to (17) we obtain

$$x^*(\hat{\theta}) = x^*(\theta) + O_p(m^{(\alpha-3)/2}),$$

so that the same error as in (18) holds also for unconstrained bootstrap, i.e.

$$F_{\hat{\theta}}(x) = F_{\theta}(x) - \phi(x^*(\theta))\Delta_1 + O_p(m^{-1}).\tag{32}$$

The steps leading from (32) to (9) are the same as those from (18) to (8).

References

- Barndorff-Nielsen, O. E. (1986). Inference on full or partial parameters based on the standardized signed log likelihood ratio. *Biometrika* 73, 307–322.
- DiCiccio, T. J., T. A. Kuffner, and G. A. Young (2017). The formal relationship between analytic and bootstrap approaches to parametric inference. *Journal of Statistical Planning and Inference* 191, 81–87.
- DiCiccio, T. J., M. A. Martin, and S. E. Stern (2001). Simple and accurate one-sided inference from signed roots of likelihood ratios. *Canadian Journal of Statistics* 29, 67–76.
- Lee, S. M. S. and G. A. Young (2005). Parametric bootstrapping with nuisance parameters. *Statistics and Probability Letters* 71, 143–153.
- Pace, L. and A. Salvan (1997). *Principles of Statistical Inference from a Neo-Fisherian Perspective*. Singapore: World Scientific.
- Pierce, D. A. and R. Bellio (2017). Modern likelihood-frequentist inference. *International Statistical Review* 85, 519–541.
- Sartori, N. (2003). Modified profile likelihoods in models with stratum nuisance parameters. *Biometrika* 90, 533–549.
- Sartori, N., R. Bellio, A. Salvan, and L. Pace (1999). The directed modified profile likelihood in models with many nuisance parameters. *Biometrika* 86, 735–742.
- Severini, T. A. (2000). *Likelihood Methods in Statistics*. Oxford: Oxford University Press.
- Young, G. A. (2009). Routes to higher-order accuracy in parametric inference. *Australian & New Zealand Journal of Statistics* 51, 115–126.
- Young, G. A. and R. L. Smith (2005). *Essentials of Statistical Inference*. Cambridge: Cambridge University Press.

Supplementary Material for Parametric bootstrap inference for stratified models with high-dimensional nuisance specifications

Ruggero Bellio^{*1}, Ioannis Kosmidis^{†2, 3}, Nicola Sartori^{‡4}, and Alessandra Salvan^{§4}

¹Department of Economics and Statistics, University of Udine, Udine, 33100, Italy

²Department of Statistics, University of Warwick, Coventry, CV4 7AL, UK

³The Alan Turing Institute, London, NW1 2DB, UK

⁴Department of Statistical Sciences, University of Padova, 35121, Padova, Italy

October 30, 2020

Full set of simulation results

In this document, we report the full set of results of the simulation studies described in the main paper. For each model, simulation results for the 23 statistics are visualized. For plotting purposes, the statistics have been split in two groups. Table [S1](#) lists the first group, and Table [S2](#) the second one.

*ruggero.bellio@uniud.it

†ioannis.kosmidis@warwick.ac.uk

‡sartori@stat.unipd.it

§salvan@stat.unipd.it

Table S1: Statistics computed in the simulation experiments (first group for plotting).

Statistic	Plotting Symbol	Description
$R(\psi)$	R	Signed likelihood root
$S(\psi)$	S	Score statistic
$T(\psi)$	T	Wald statistic
$\Phi^{-1}\{\hat{p}_1^T(\psi)\}$	T^u	Transformed p -value from unconstrained bootstrap of $T(\psi)$
$\Phi^{-1}\{\hat{p}_2^T(\psi)\}$	T^c	Transformed p -value from constrained bootstrap of $T(\psi)$
$\Phi^{-1}\{\hat{p}_1^S(\psi)\}$	S^u	Transformed p -value from unconstrained bootstrap of $S(\psi)$
$\Phi^{-1}\{\hat{p}_2^S(\psi)\}$	S^c	Transformed p -value from constrained bootstrap of $S(\psi)$
$\Phi^{-1}\{\hat{p}_1^R(\psi)\}$	R^u	Transformed p -value from unconstrained bootstrap of $R(\psi)$
$\Phi^{-1}\{\hat{p}_2^R(\psi)\}$	R^c	Transformed p -value from constrained bootstrap of $R(\psi)$
$R^*(\psi)$	R^*	Modified signed likelihood root
$R_m(\psi)$	R_m	Signed likelihood root computed from the modified profile likelihood

Table S2: Statistics computed in the simulation experiments (second group for plotting). The mean $\hat{\mu}^R$ and the standard deviation $\hat{\sigma}^R$ of $R(\psi)$ are estimated through unconstrained bootstrap, by simulating from the model at $\theta = \hat{\theta}$, and likewise for $S(\psi)$ and $T(\psi)$. The mean $\tilde{\mu}^R$ and the standard deviation $\tilde{\sigma}^R$ of $R(\psi)$ are estimated through constrained bootstrap, by simulating from the model at $\theta = \hat{\theta}_\psi$, and likewise for $S(\psi)$ and $T(\psi)$.

Statistic	Plotting Symbol	Description
$T(\psi) - \hat{\mu}^T$	T_l^u	Location adjusted $T(\psi)$, unconstrained bootstrap
$T(\psi) - \tilde{\mu}^T$	T_l^c	Location adjusted $T(\psi)$, constrained bootstrap
$S(\psi) - \hat{\mu}^S$	S_l^u	Location adjusted $S(\psi)$, unconstrained bootstrap
$S(\psi) - \tilde{\mu}^S$	S_l^c	Location adjusted $S(\psi)$, constrained bootstrap
$R(\psi) - \hat{\mu}^R$	R_l^u	Location adjusted $R(\psi)$, unconstrained bootstrap
$R(\psi) - \tilde{\mu}^R$	R_l^c	Location adjusted $R(\psi)$, constrained bootstrap
$(T(\psi) - \hat{\mu}^T)/\tilde{\sigma}^T$	T_{ls}^u	Location-and-scale adjusted $T(\psi)$, unconstrained bootstrap
$(T(\psi) - \tilde{\mu}^T)/\tilde{\sigma}^T$	T_{ls}^c	Location-and-scale adjusted $T(\psi)$, constrained bootstrap
$(S(\psi) - \hat{\mu}^S)/\tilde{\sigma}^S$	S_{ls}^u	Location-and-scale adjusted $S(\psi)$, unconstrained bootstrap
$(S(\psi) - \tilde{\mu}^S)/\tilde{\sigma}^S$	S_{ls}^c	Location-and-scale adjusted $S(\psi)$, constrained bootstrap
$(R(\psi) - \hat{\mu}^R)/\tilde{\sigma}^R$	R_{ls}^u	Location-and-scale adjusted $R(\psi)$, unconstrained bootstrap
$(R(\psi) - \tilde{\mu}^R)/\tilde{\sigma}^R$	R_{ls}^c	Location-and-scale adjusted $R(\psi)$, constrained bootstrap

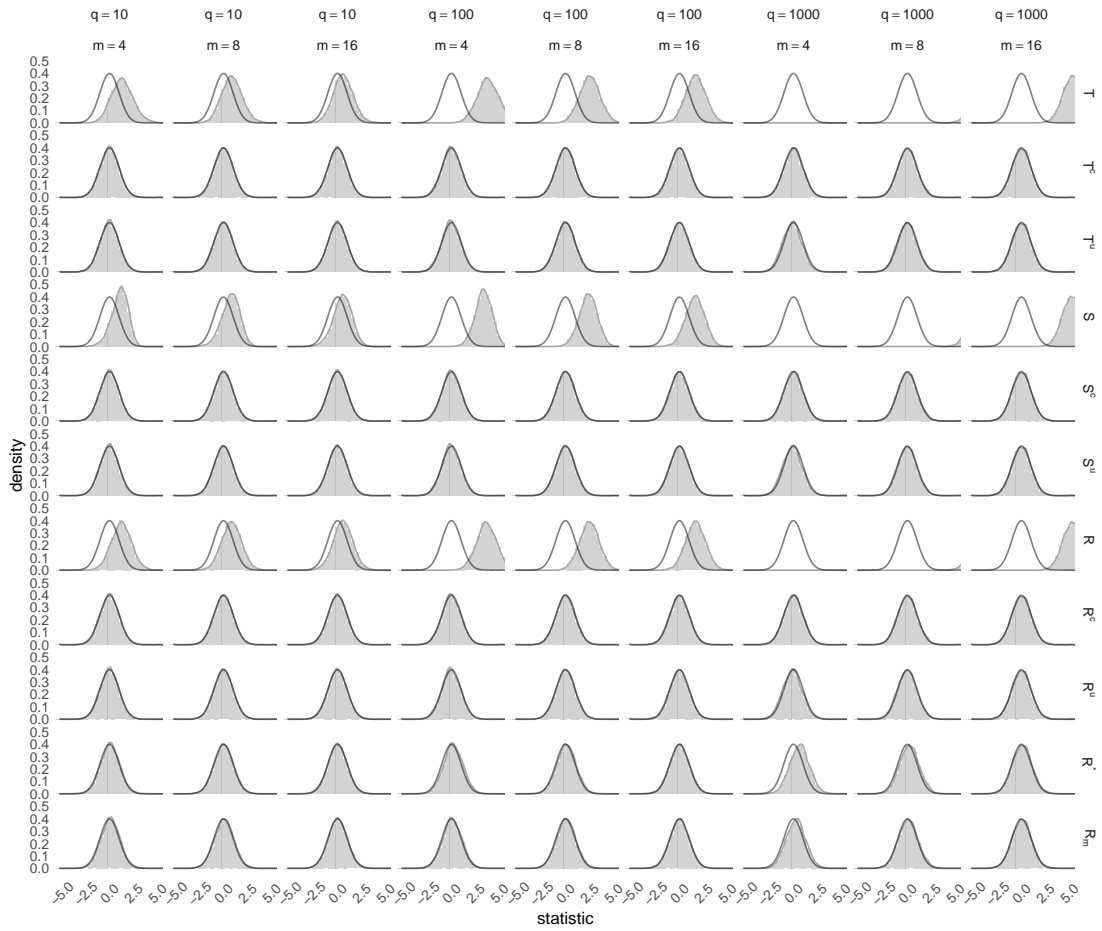


Figure S1: Gamma model. Estimated null distribution of statistics for the statistics in Table S1 for various combinations of q and m . The $N(0,1)$ density function is superimposed.

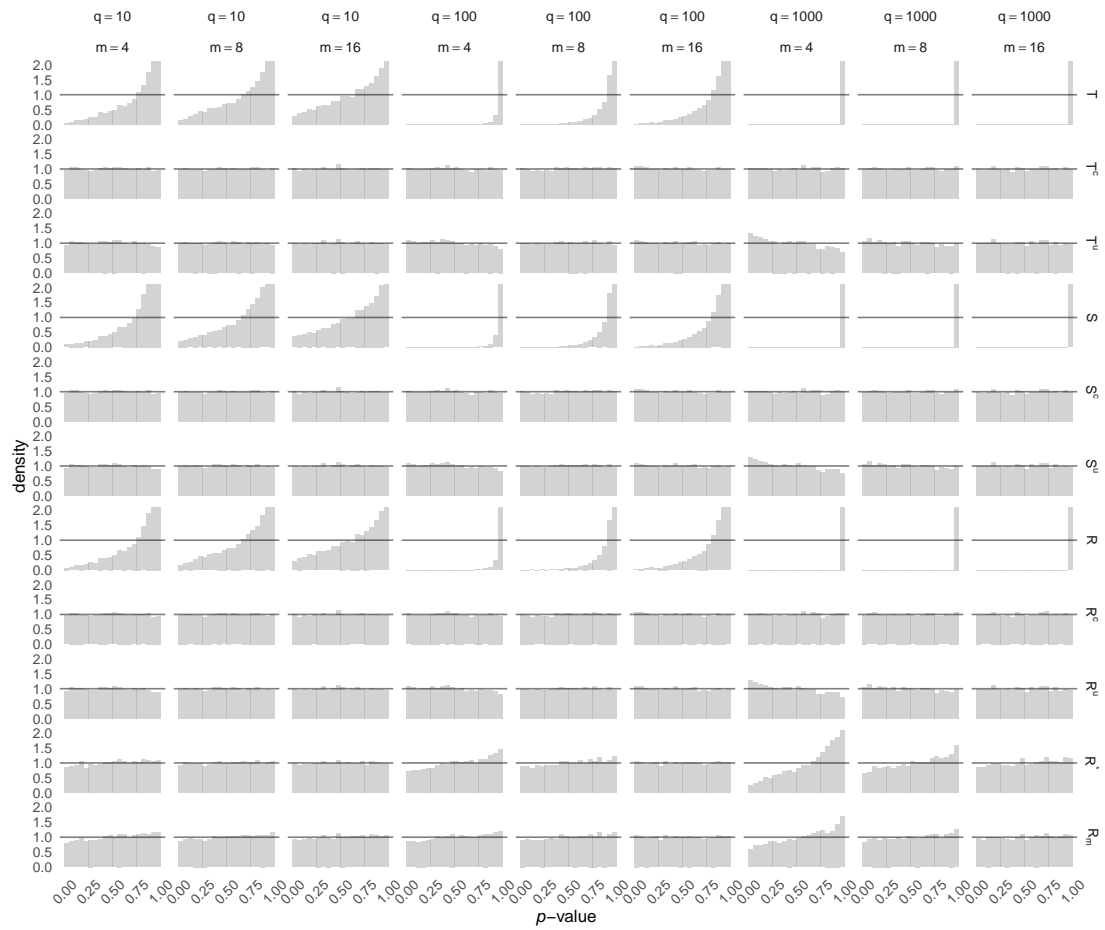


Figure S2: Gamma model. Estimated distribution of p -values for the statistics in Table S1 for various combinations of q and m . The Uniform(0,1) density function is superimposed.

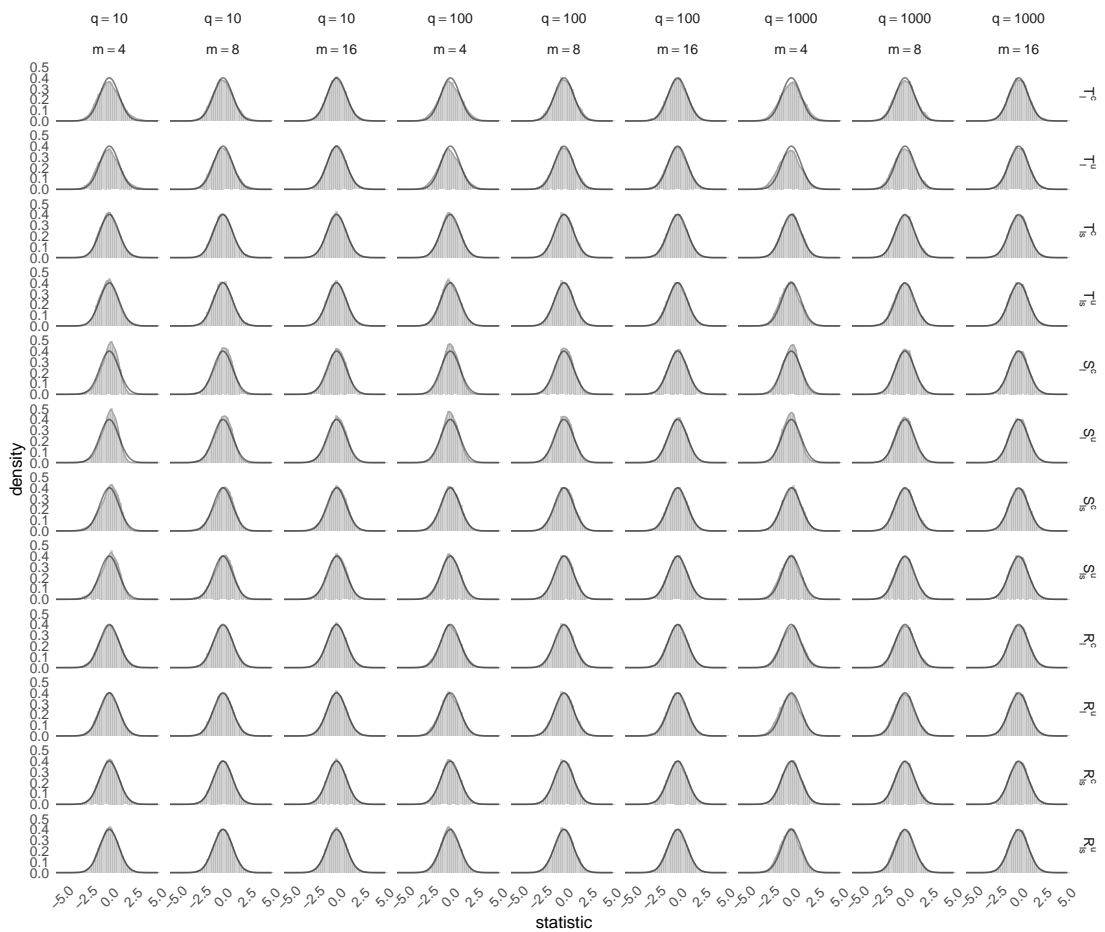


Figure S3: Gamma model. Estimated null distribution of statistics for the statistics in Table S2 for various combinations of q and m . The $N(0,1)$ density function is superimposed.

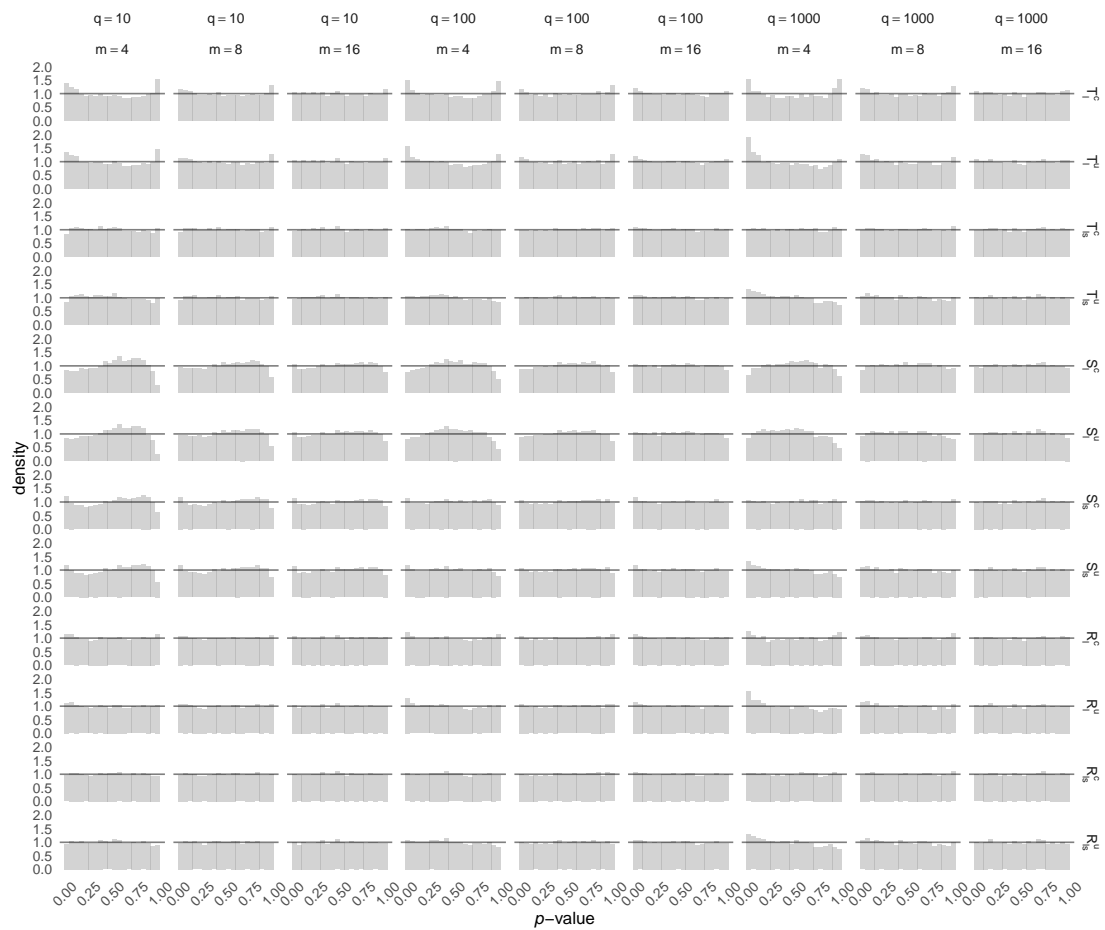


Figure S4: Gamma model. Estimated null distribution of p -values for the statistics in Table S2 for various combinations of q and m . The Uniform(0,1) density function is superimposed.

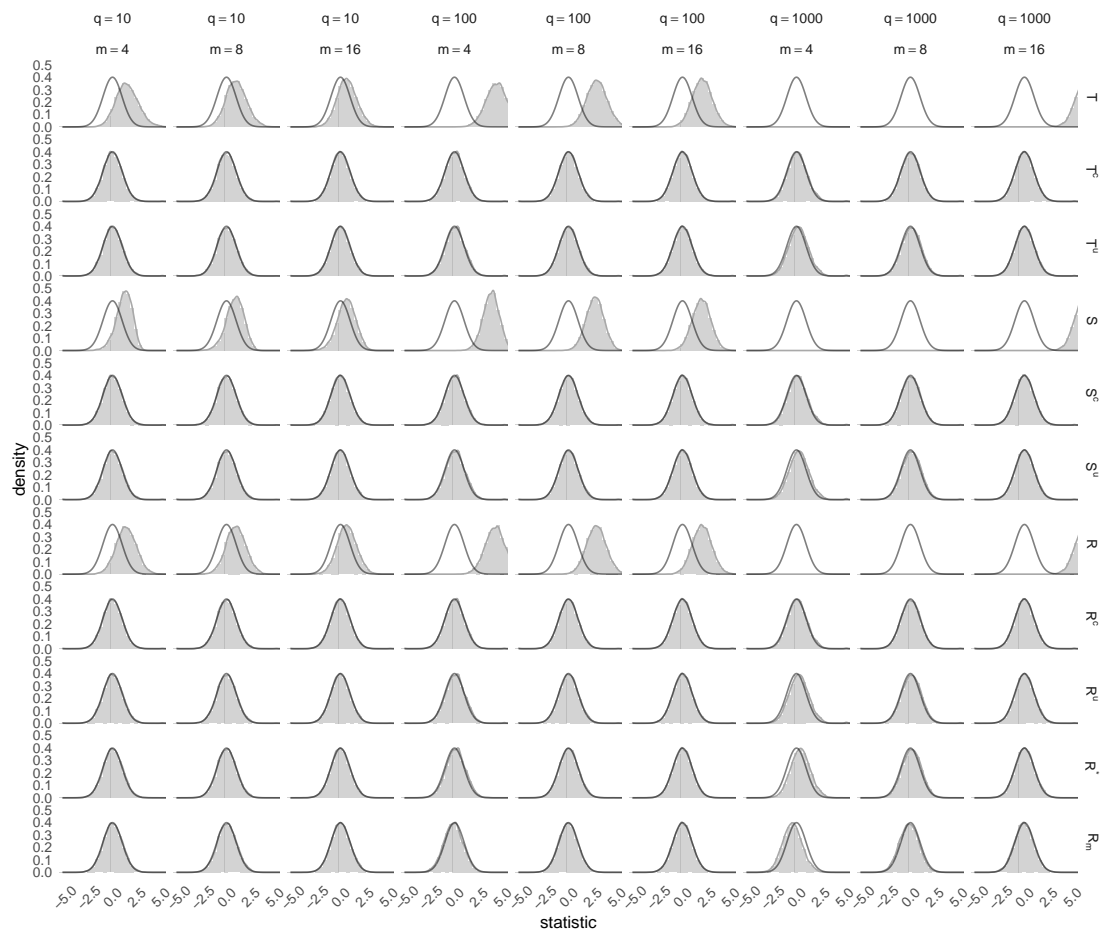


Figure S5: Beta model. Estimated null distribution of statistics for the statistics in Table S1 for various combinations of q and m . The $N(0,1)$ density function is superimposed.

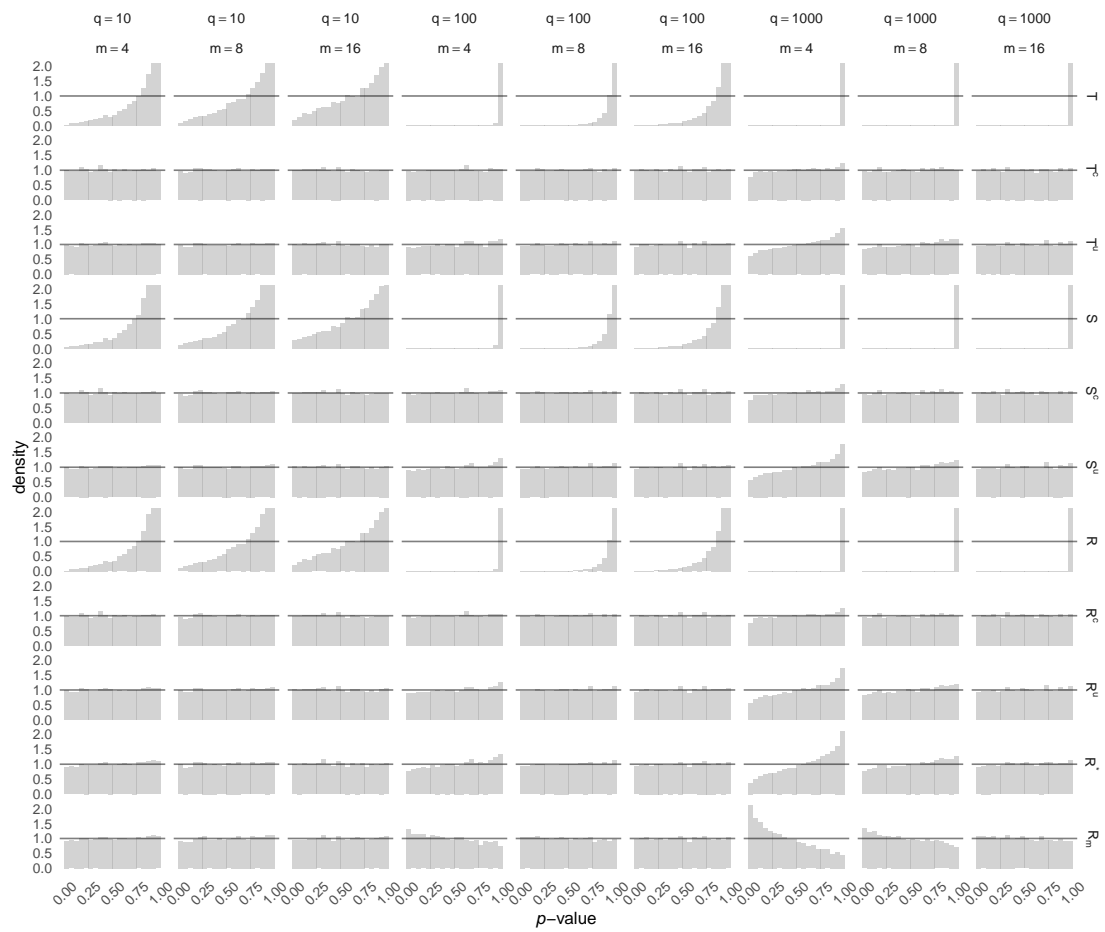


Figure S6: Beta model. Estimated distribution of p -values for the statistics in Table S1 for various combinations of q and m . The Uniform(0,1) density function is superimposed.

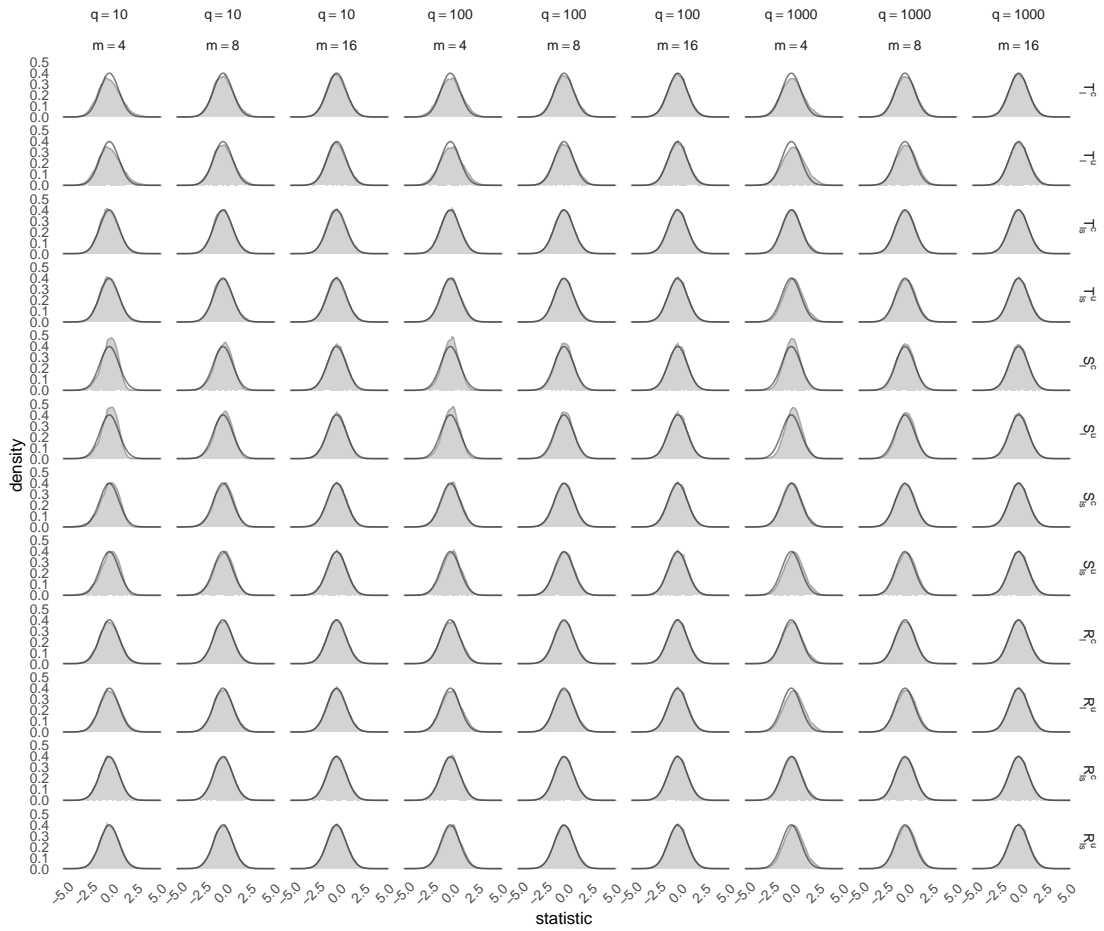


Figure S7: Beta model. Estimated null distribution of statistics for the statistics in Table S2 for various combinations of q and m . The $N(0,1)$ density function is superimposed.

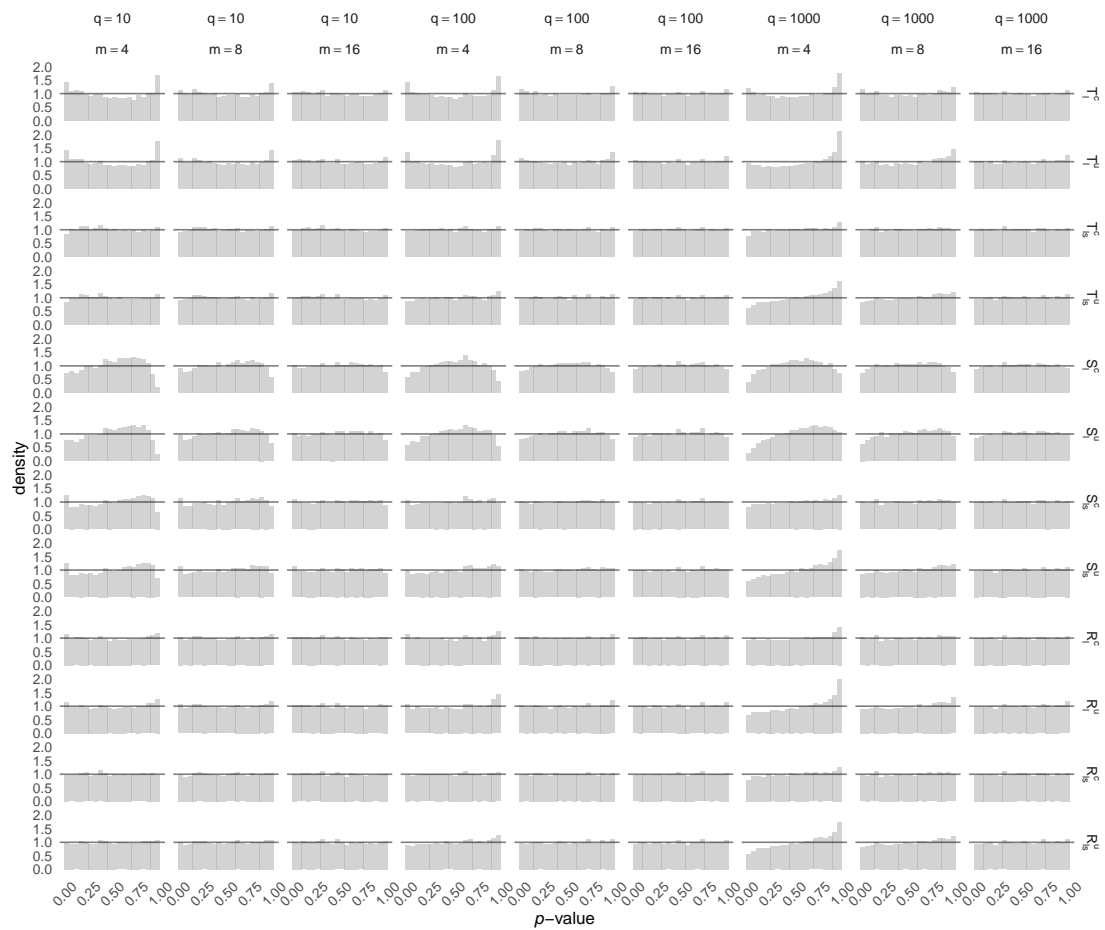


Figure S8: Beta model. Estimated null distribution of p -values for the statistics in Table S2 for various combinations of q and m . The Uniform(0,1) density function is superimposed.

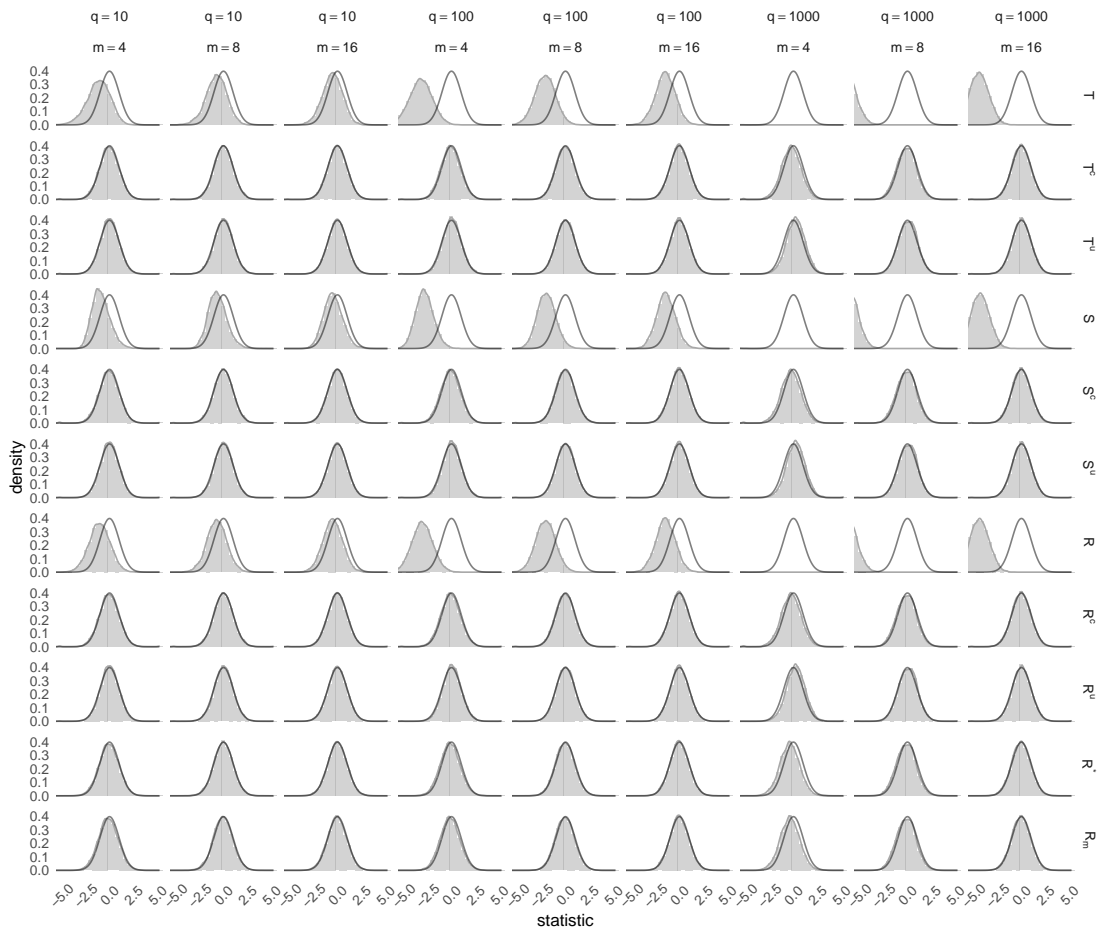


Figure S9: Curved exponential family. Estimated null distribution of statistics for the statistics in Table S1 for various combinations of q and m . The $N(0,1)$ density function is superimposed.

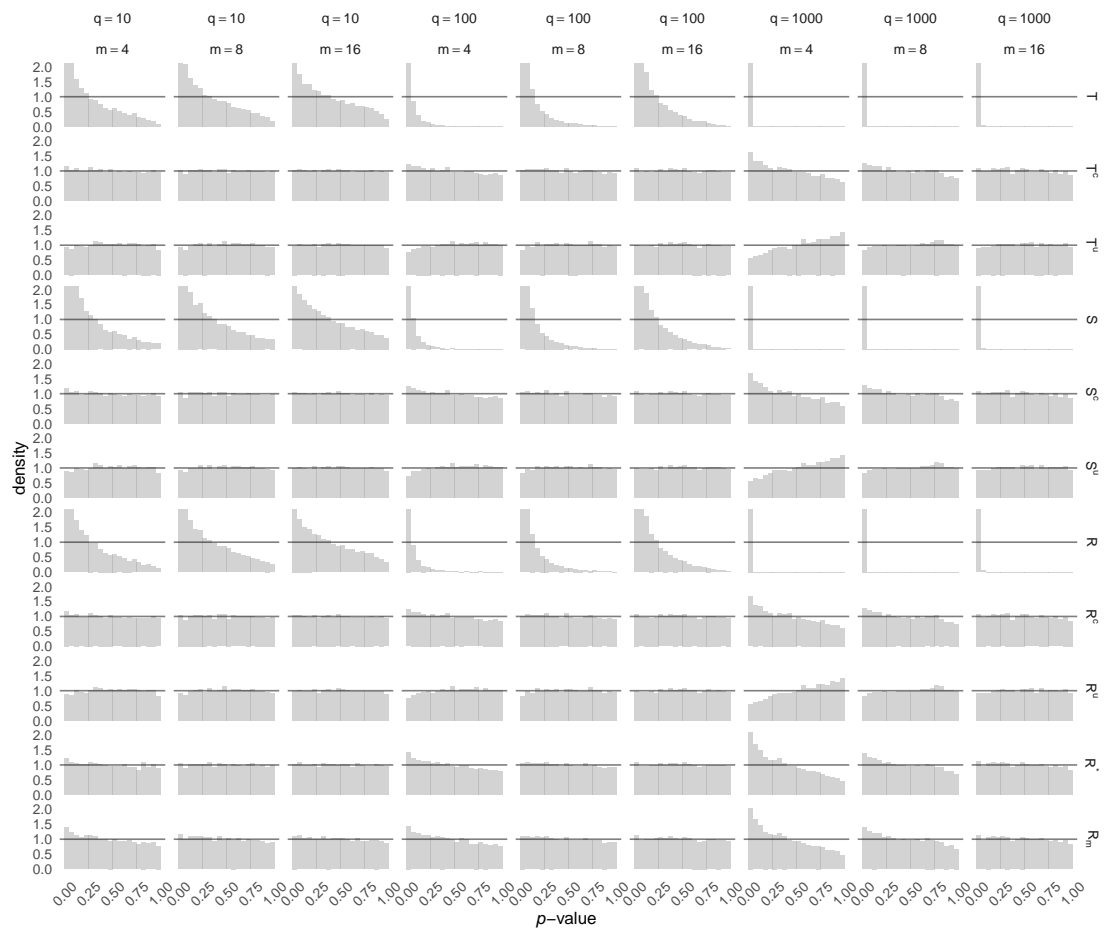


Figure S10: Curved exponential family. Estimated distribution of p -values for the statistics in Table S1 for various combinations of q and m . The Uniform(0,1) density function is superimposed.

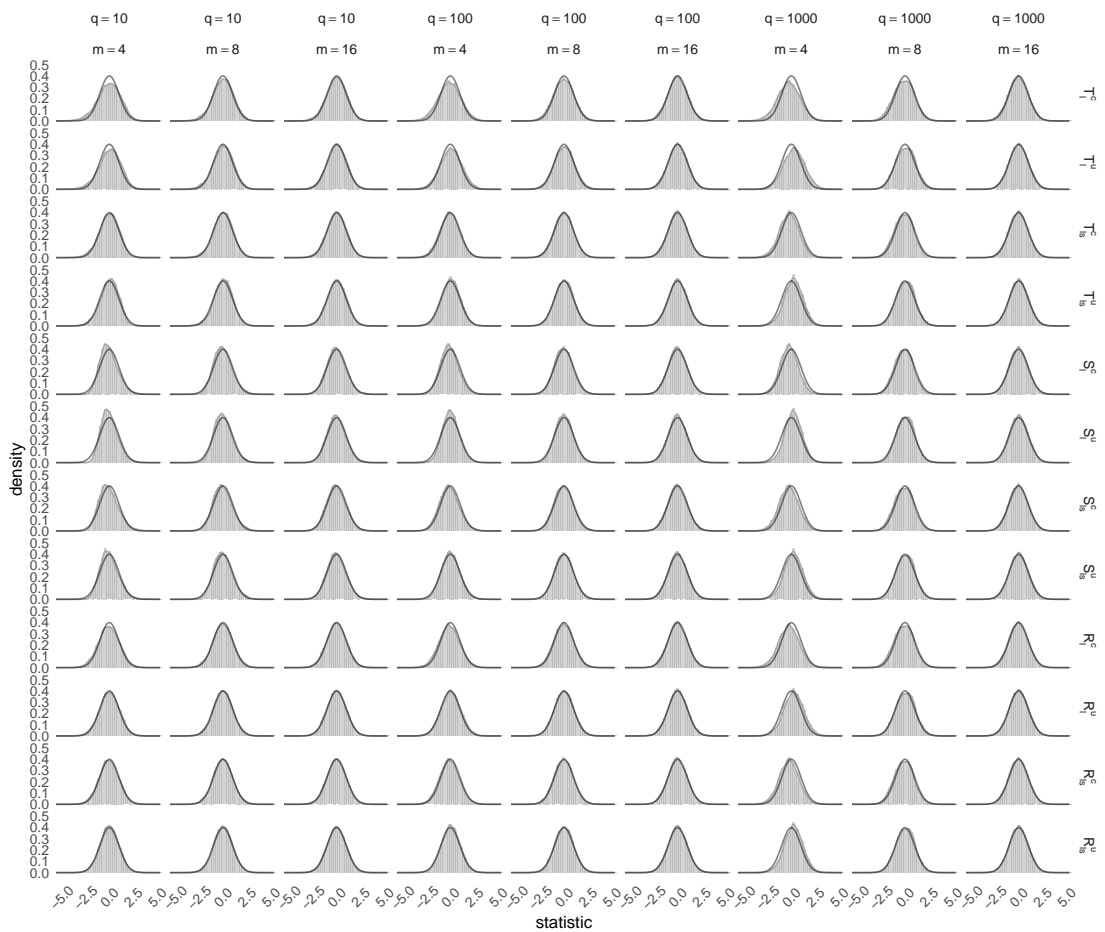


Figure S11: Curved exponential family. Estimated null distribution of statistics for the statistics in Table S2 for various combinations of q and m . The $N(0,1)$ density function is superimposed.

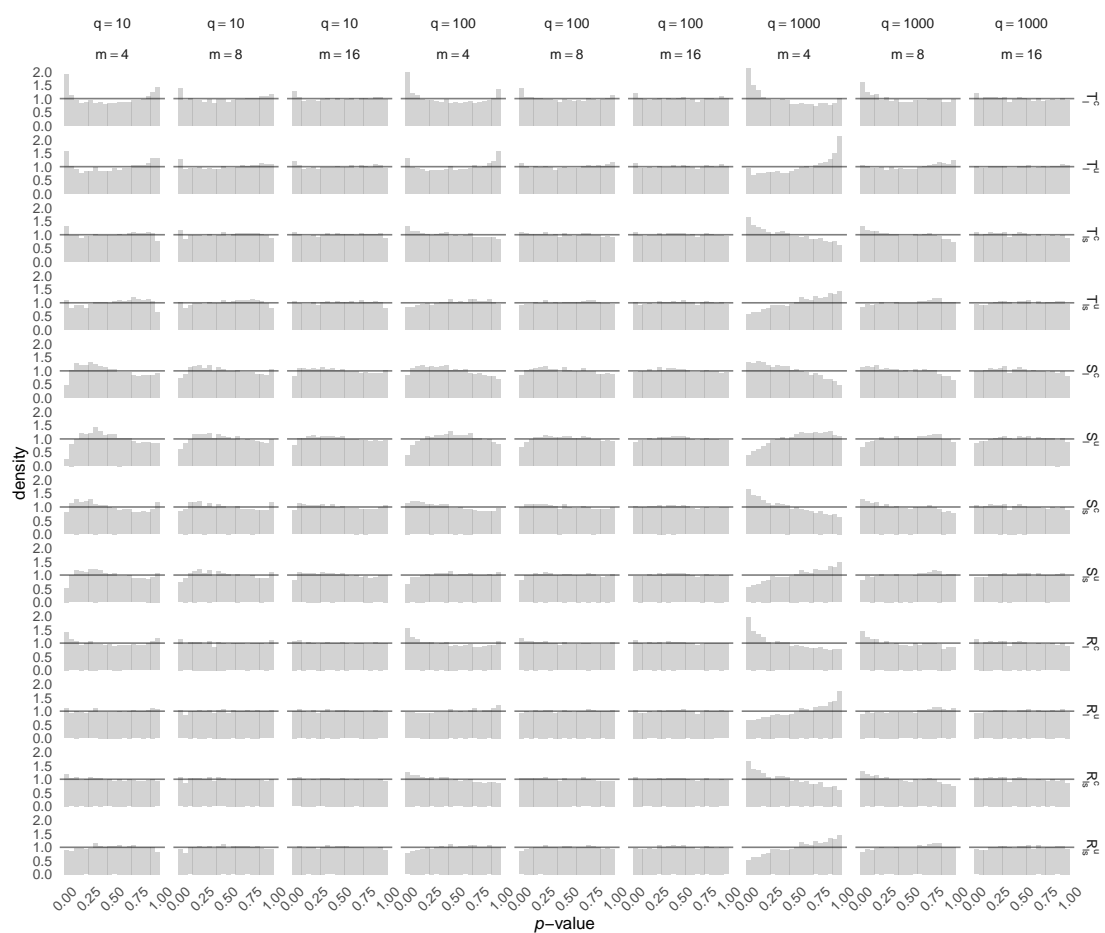


Figure S12: Curved exponential family. Estimated null distribution of p -values for the statistics in Table S2 for various combinations of q and m . The Uniform(0,1) density function is superimposed.

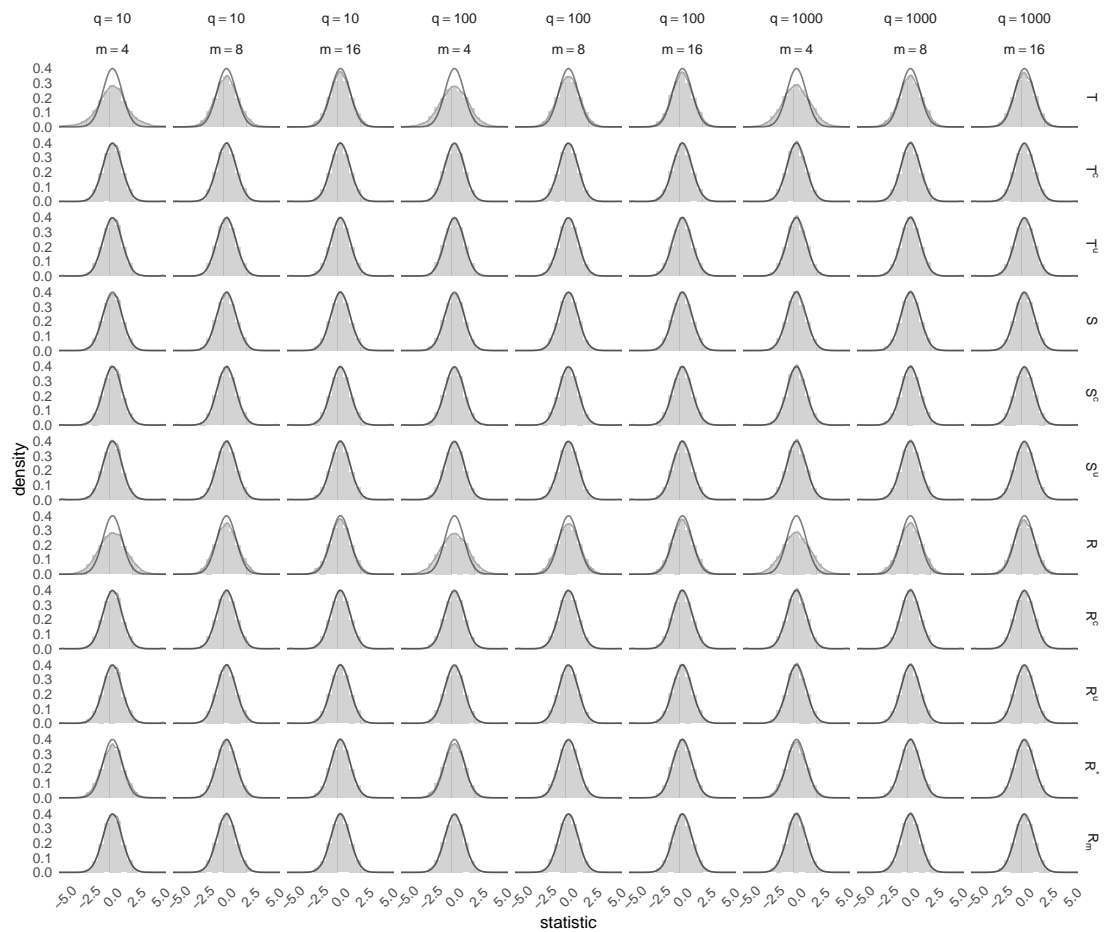


Figure S13: Behrens-Fisher model. Estimated null distribution of statistics for the statistics in Table S1 for various combinations of q and m . The $N(0,1)$ density function is superimposed.

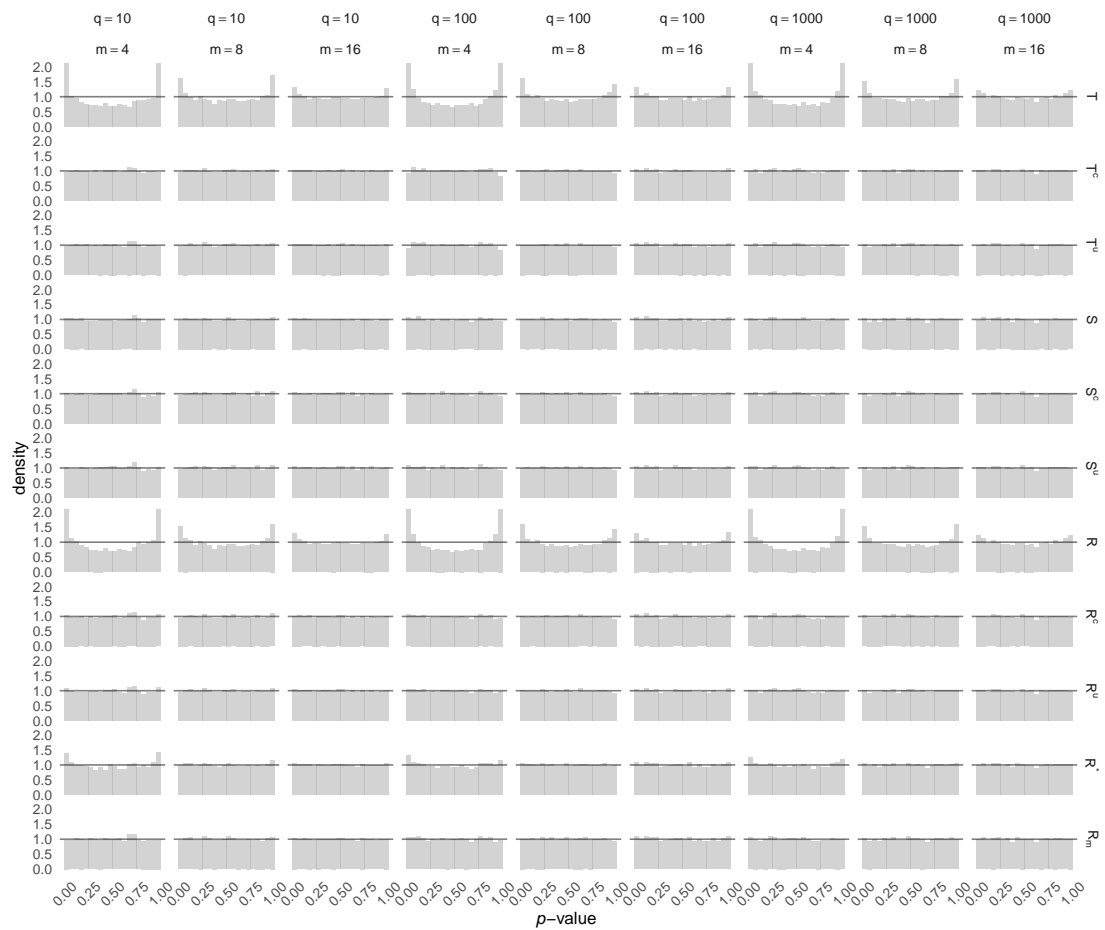


Figure S14: Behrens-Fisher model. Estimated distribution of p -values for the statistics in Table S1 for various combinations of q and m . The Uniform(0,1) density function is superimposed.

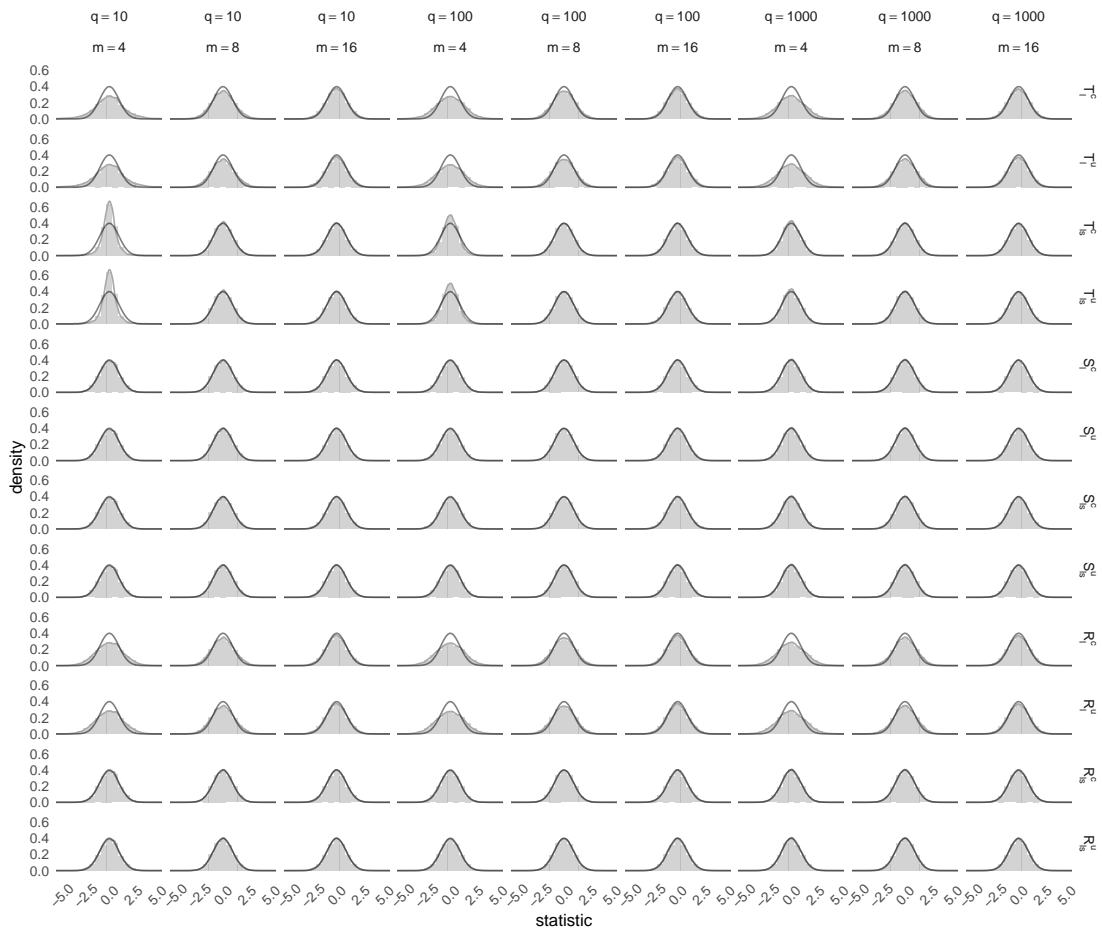


Figure S15: Behrens-Fisher model. Estimated null distribution of statistics for the statistics in Table S2 for various combinations of q and m . The $N(0,1)$ density function is superimposed.

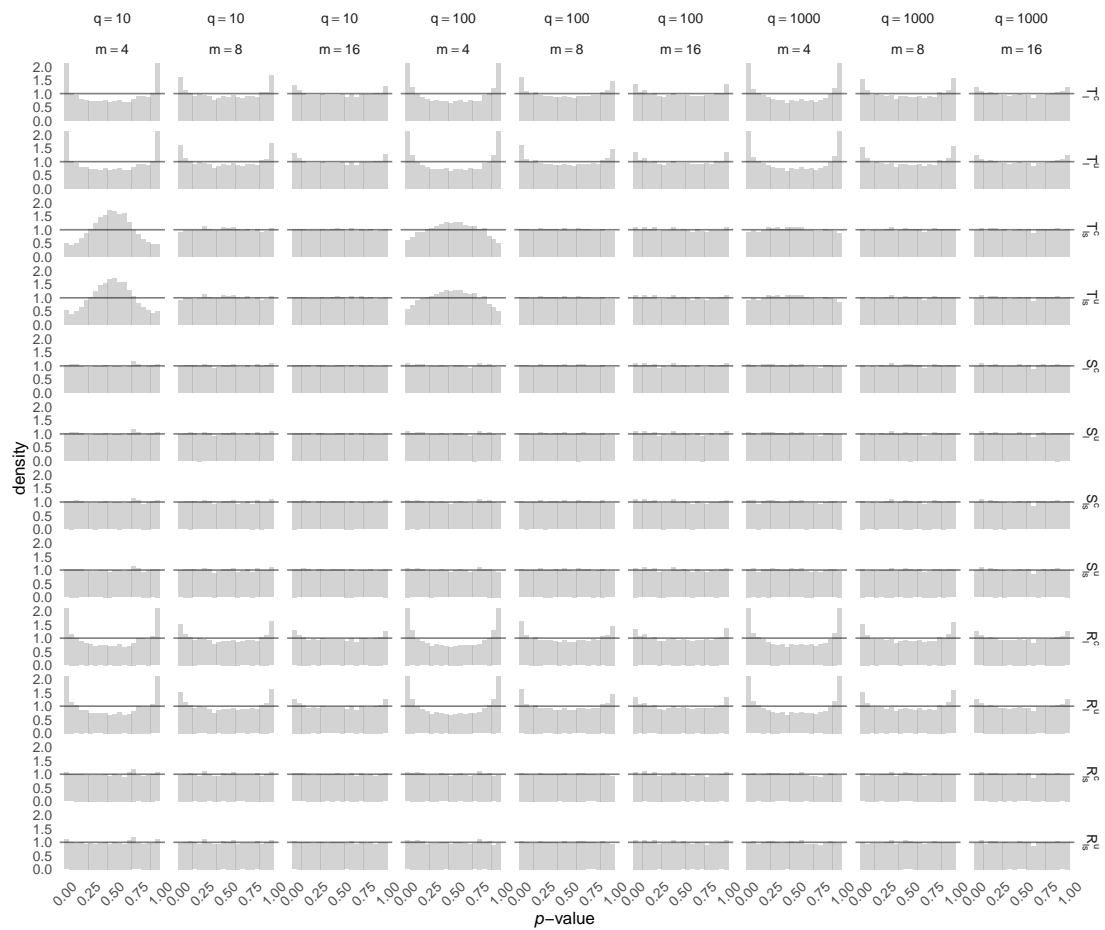


Figure S16: Behrens-Fisher model. Estimated null distribution of p -values for the statistics in Table S2 for various combinations of q and m . The Uniform(0,1) density function is superimposed.

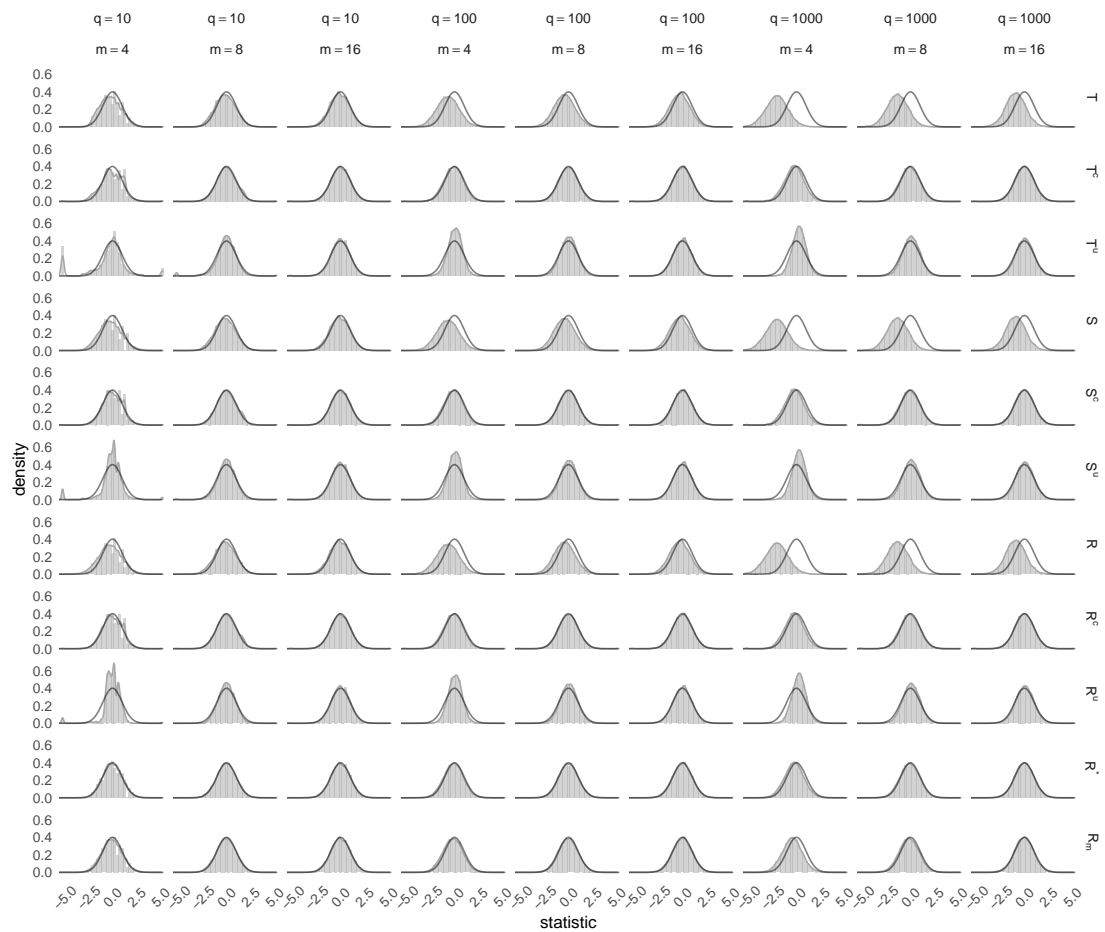


Figure S17: Logistic regression example. Estimated null distribution of statistics for the statistics in Table S1 for various combinations of q and m . The $N(0,1)$ density function is superimposed.

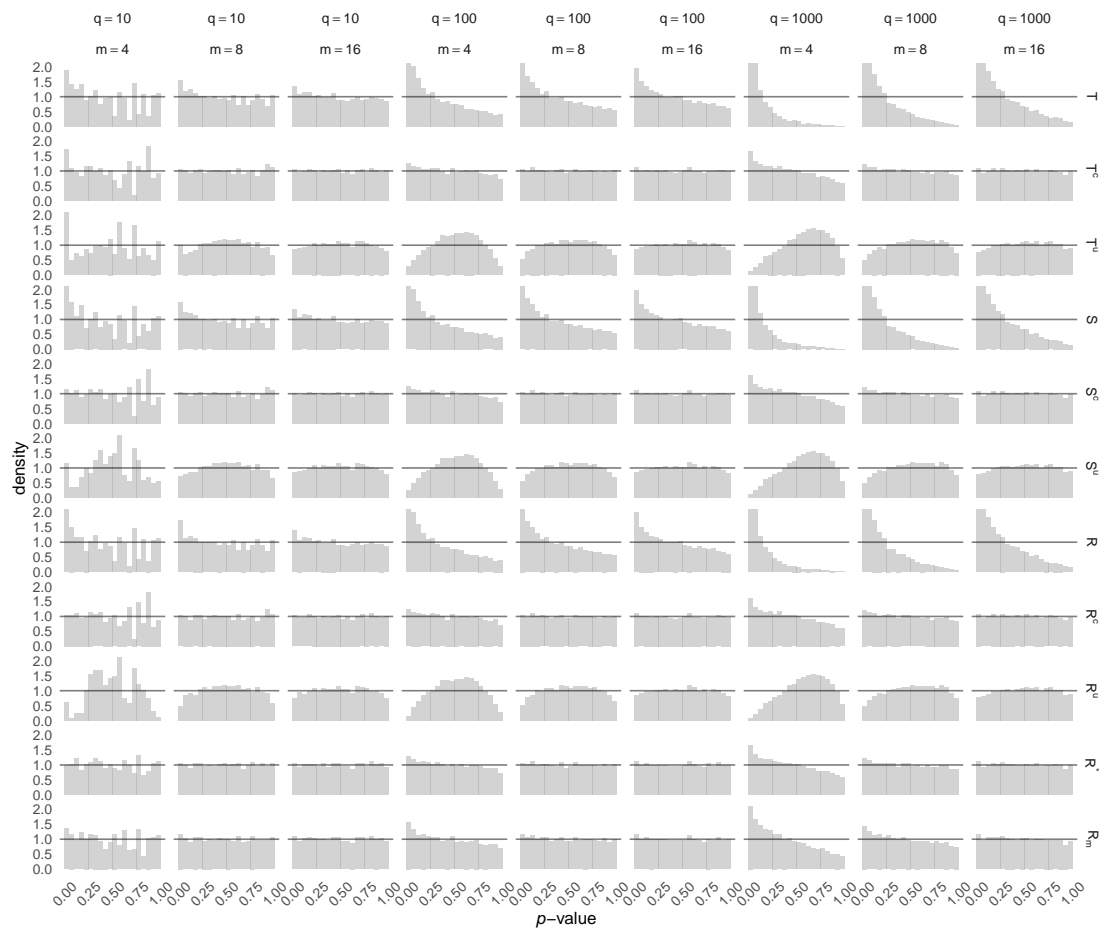


Figure S18: Logistic regression example. Estimated distribution of p -values for the statistics in Table S1 for various combinations of q and m . The Uniform(0,1) density function is superimposed.

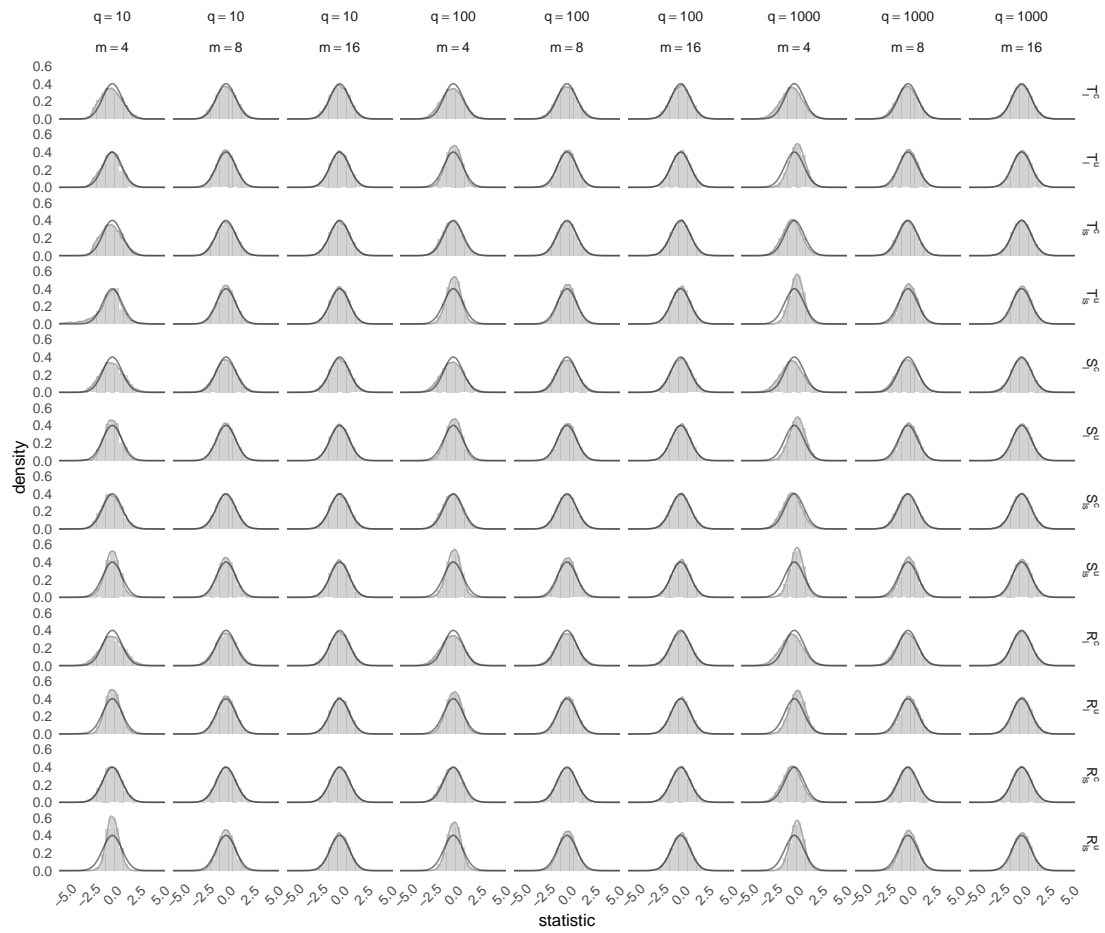


Figure S19: Logistic regression example. Estimated null distribution of statistics for the statistics in Table S2 for various combinations of q and m . The $N(0,1)$ density function is superimposed.

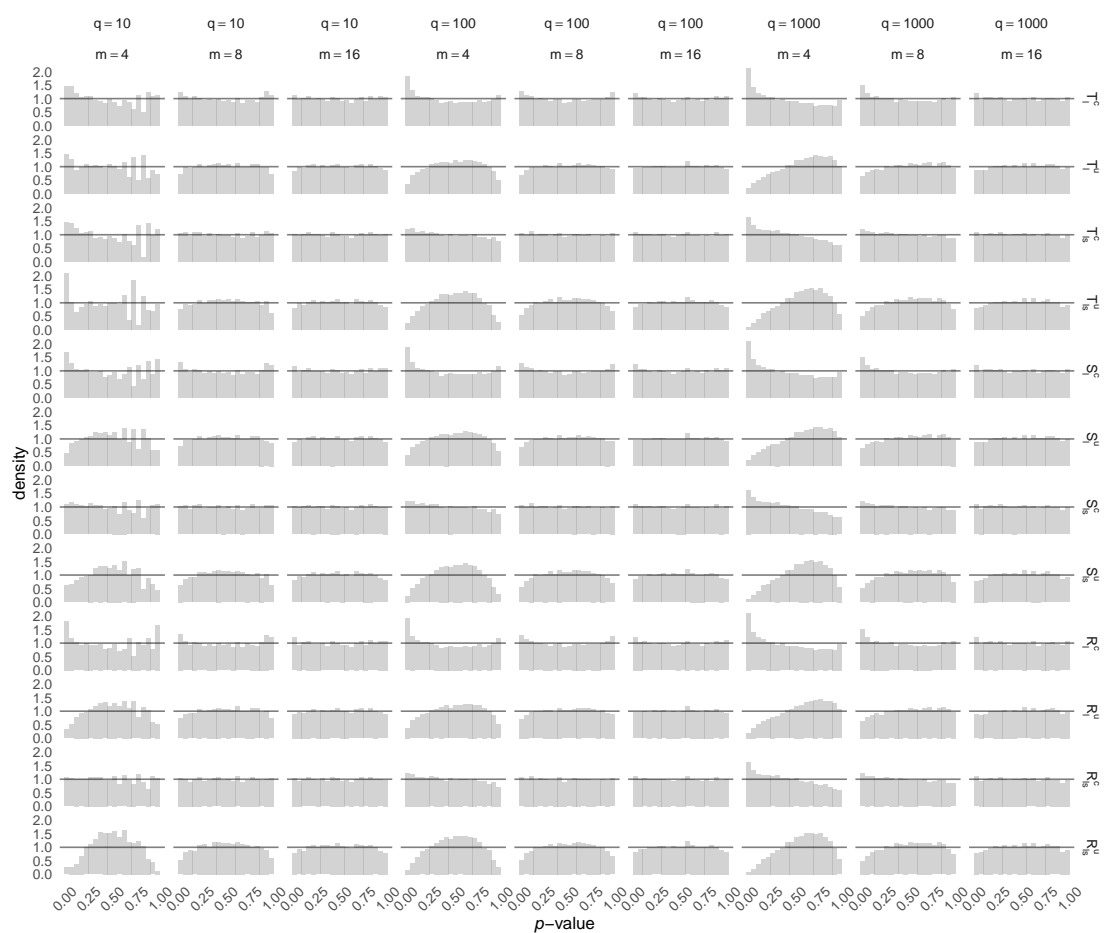


Figure S20: Logistic regression example. Estimated null distribution of p -values for the statistics in Table S2 for various combinations of q and m . The Uniform(0,1) density function is superimposed.

Empirical tail probabilities

The following tables report empirical tail probabilities for the statistics in Table 1 of the main text, for all models and all simulation settings. The rows of each table are subdivided into 5 different blocks, each one corresponding to a different model.

Table S3: Empirical tail probabilities $\times 100$ for the statistics in Table 1 of the main text and all models that have been considered in the simulation experiments. The figures shown have been rounded to 1 decimal and are for $q = 10$ and $m = 4$.

Model	Statistic	Nominal					
		1.0	2.5	5.0	95.0	97.5	99.0
Gamma	R	0.1	0.1	0.3	65.2	75.6	85.3
	R^*	0.8	2.2	4.3	94.5	97.1	98.8
	R^u	1.0	2.5	4.7	95.6	97.7	99.2
	R^c	1.0	2.5	4.8	95.3	97.7	99.0
	R_l^c	1.5	3.1	5.6	94.4	96.9	98.7
	R_{ls}^c	1.0	2.5	4.8	95.3	97.5	99.0
Beta	R	0.0	0.0	0.1	58.5	69.3	80.1
	R^*	0.9	2.1	4.5	94.6	97.1	98.7
	R^u	1.0	2.4	5.0	94.7	97.2	98.8
	R^c	0.9	2.4	4.9	95.1	97.5	99.0
	R_l^c	1.2	2.8	5.8	94.2	96.8	98.5
	R_{ls}^c	0.9	2.3	4.9	95.1	97.5	98.9
Curved exponential family	R	11.8	19.4	28.1	99.4	99.8	99.9
	R^*	1.4	3.2	6.1	95.6	97.6	99.0
	R^u	0.8	2.1	4.4	95.8	98.0	99.2
	R^c	1.4	3.0	5.9	95.3	97.6	99.0
	R_l^c	1.9	4.1	7.1	94.2	96.9	98.6
	R_{ls}^c	1.4	3.1	6.0	95.4	97.6	99.0
Behrens-Fisher	R	4.9	8.0	12.1	88.0	91.8	95.1
	R^*	1.9	4.0	7.0	92.9	96.0	98.1
	R^u	1.4	2.9	5.4	94.4	97.0	98.8
	R^c	1.1	2.7	5.2	94.7	97.3	98.9
	R_l^c	4.9	7.9	12.1	87.9	91.8	95.1
	R_{ls}^c	1.0	2.6	5.3	94.7	97.4	99.0
Logistic regression	R	3.8	7.1	12.5	94.4	97.0	98.4
	R^*	0.5	2.2	5.0	94.4	97.1	98.7
	R^u	2.1	2.6	3.1	99.4	99.6	99.7
	R^c	0.8	2.4	5.2	95.6	97.6	99.0
	R_l^c	2.9	5.5	9.1	91.7	94.5	97.2
	R_{ls}^c	1.0	2.6	5.3	94.8	97.3	99.0

Table S4: Empirical tail probabilities $\times 100$ for the statistics in Table 1 of the main text and all models that have been considered in the simulation experiments. The figures shown have been rounded to 1 decimal and are for $q = 10$ and $m = 8$.

Model	Statistic	Nominal					
		1.0	2.5	5.0	95.0	97.5	99.0
Gamma	R	0.1	0.3	0.9	78.6	86.5	92.8
	R^*	0.9	2.3	4.6	94.7	97.4	98.8
	R^u	1.0	2.4	4.9	95.2	97.7	99.1
	R^c	1.0	2.5	4.9	95.0	97.5	99.0
	R_l^c	1.2	2.8	5.4	94.4	97.2	98.7
	R_{ls}^c	1.0	2.5	4.9	95.0	97.5	98.9
Beta	R	0.1	0.2	0.5	73.8	82.8	90.5
	R^*	0.9	2.3	4.9	94.7	97.1	98.9
	R^u	0.9	2.4	4.9	94.5	97.1	98.8
	R^c	0.9	2.4	4.8	94.8	97.4	99.0
	R_l^c	1.0	2.6	5.2	94.4	96.9	98.8
	R_{ls}^c	0.9	2.3	4.9	94.8	97.2	98.9
Curved exponential family	R	5.8	10.5	17.4	98.8	99.5	99.8
	R^*	1.1	3.0	5.3	95.1	97.5	99.0
	R^u	0.9	2.3	4.5	95.4	97.7	99.3
	R^c	1.1	2.9	5.2	95.0	97.4	99.1
	R_l^c	1.3	3.3	5.8	94.5	97.1	98.8
	R_{ls}^c	1.1	3.0	5.3	95.0	97.4	99.1
Behrens-Fisher	R	2.0	4.3	7.6	92.0	95.2	97.6
	R^*	1.0	2.5	5.0	94.3	97.0	99.0
	R^u	1.0	2.3	4.8	94.5	97.3	99.1
	R^c	1.0	2.3	4.8	94.5	97.3	99.2
	R_l^c	2.0	4.3	7.6	91.9	95.2	97.6
	R_{ls}^c	0.9	2.4	4.9	94.5	97.2	99.0
Logistic regression	R	2.2	4.7	8.6	94.8	97.0	99.1
	R^*	0.9	2.7	5.3	94.8	97.0	99.1
	R^u	0.1	0.7	2.4	97.2	98.9	99.6
	R^c	0.9	2.6	5.2	94.5	97.9	99.1
	R_l^c	1.6	3.6	6.7	94.0	96.9	98.4
	R_{ls}^c	0.9	2.6	5.2	94.8	97.4	99.0

Table S5: Empirical tail probabilities $\times 100$ for the statistics in Table 1 of the main text and all models that have been considered in the simulation experiments. The figures shown have been rounded to 1 decimal and are for $q = 10$ and $m = 16$.

Model	Statistic	Nominal						
		1.0	2.5	5.0	95.0	97.5	99.0	
Gamma	R	0.2	0.6	1.5	85.7	91.6	96.0	
	R^*	1.1	2.5	4.9	95.0	97.4	98.9	
	R^u	1.0	2.6	5.0	95.2	97.5	99.0	
	R^c	1.1	2.6	5.1	95.1	97.5	99.0	
	R_l^c	1.2	2.8	5.3	94.9	97.3	98.9	
	R_{ls}^c	1.2	2.6	5.1	95.1	97.4	98.9	
Beta	R	0.2	0.4	1.1	83.4	89.8	94.8	
	R^*	1.0	2.4	5.0	94.9	97.5	99.1	
	R^u	1.1	2.6	5.1	94.8	97.4	99.0	
	R^c	1.0	2.4	5.0	95.0	97.5	99.1	
	R_l^c	1.0	2.5	5.1	94.9	97.3	99.0	
	R_{ls}^c	1.0	2.4	5.0	95.0	97.5	99.1	
Curved exponential family	R	3.7	7.7	13.1	98.4	99.2	99.8	
	R^*	1.1	2.7	5.1	95.3	97.8	99.1	
	R^u	1.0	2.4	4.9	95.5	97.9	99.2	
	R^c	1.1	2.6	5.2	95.3	97.8	99.1	
	R_l^c	1.3	3.3	5.8	94.5	97.1	98.8	
	R_{ls}^c	1.1	3.0	5.3	95.0	97.4	99.1	
Behrens-Fisher	R	1.8	3.5	6.4	93.7	96.7	98.6	
	R^*	1.2	2.9	5.3	94.8	97.4	99.0	
	R^u	1.2	2.8	5.2	94.9	97.5	99.1	
	R^c	1.2	2.8	5.1	94.9	97.5	99.1	
	R_l^c	1.8	3.5	6.4	93.8	96.6	98.6	
	R_{ls}^c	1.2	2.9	5.1	94.9	97.4	99.1	
Logistic regression	R	1.7	3.7	7.0	95.7	98.0	99.3	
	R^*	1.0	2.7	5.2	95.4	97.7	99.3	
	R^u	0.6	1.8	3.8	96.3	98.4	99.5	
	R^c	1.0	2.6	5.1	94.9	97.5	99.0	
	R_l^c	1.2	3.1	6.0	94.6	97.2	98.9	
	R_{ls}^c	1.0	2.7	5.2	95.1	97.6	99.1	

Table S6: Empirical tail probabilities $\times 100$ for the statistics in Table 1 of the main text and all models that have been considered in the simulation experiments. The figures shown have been rounded to 1 decimal and are for $q = 100$ and $m = 4$.

Model	Statistic	Nominal					
		1.0	2.5	5.0	95.0	97.5	99.0
Gamma	R	0.0	0.0	0.0	2.7	5.2	10.0
	R^*	0.6	1.6	3.5	92.8	96.2	98.4
	R^u	1.0	2.8	5.4	95.9	98.0	99.3
	R^c	0.9	2.6	5.2	95.2	97.6	99.1
	R_l^c	1.3	3.4	6.1	94.2	96.9	98.7
	R_{ls}^c	1.0	2.6	5.2	95.2	97.5	99.1
Beta	R	0.0	0.0	0.0	0.7	1.4	3.4
	R^*	0.8	2.0	3.8	93.4	96.7	98.7
	R^u	0.9	2.3	4.5	93.7	97.0	98.7
	R^c	0.9	2.5	4.9	94.8	97.4	99.1
	R_l^c	1.3	2.9	5.7	93.8	96.9	98.7
	R_{ls}^c	1.0	2.5	4.9	94.7	97.5	99.0
Curved exponential family	R	75.1	84.2	90.3	100.0	100.0	100.0
	R^*	1.6	3.7	7.1	96.0	97.9	99.2
	R^u	0.7	1.7	3.7	95.0	97.5	99.0
	R^c	1.3	3.2	6.2	95.7	97.8	99.1
	R_l^c	1.8	4.2	7.7	94.7	97.2	98.7
	R_{ls}^c	1.5	3.3	6.3	95.7	97.7	99.1
Behrens-Fisher	R	5.2	8.8	12.8	88.5	92.2	95.2
	R^*	1.7	3.5	6.7	94.2	96.8	98.6
	R^u	1.2	2.8	5.3	95.1	97.7	98.9
	R^c	1.1	2.8	5.3	95.2	97.7	99.0
	R_l^c	5.3	8.9	12.8	88.4	92.2	95.3
	R_{ls}^c	1.1	2.8	5.3	95.2	97.7	99.0
Logistic regression	R	8.1	14.0	20.5	98.0	99.0	99.5
	R^*	1.4	3.2	6.4	96.4	98.1	99.2
	R^u	0.1	0.2	0.8	98.6	99.6	99.9
	R^c	1.3	3.2	6.2	96.4	98.2	99.2
	R_l^c	2.8	5.7	9.5	94.2	96.8	98.3
	R_{ls}^c	1.3	3.2	6.1	96.4	98.1	99.2

Table S7: Empirical tail probabilities $\times 100$ for the statistics in Table 1 of the main text and all models that have been considered in the simulation experiments. The figures shown have been rounded to 1 decimal and are for $q = 100$ and $m = 8$.

Model	Statistic	Nominal					
		1.0	2.5	5.0	95.0	97.5	99.0
Gamma	R	0.0	0.0	0.0	20.5	29.8	43.5
	R^*	0.8	2.0	4.4	93.8	97.1	98.9
	R^u	0.9	2.4	5.0	95.2	97.8	99.1
	R^c	1.1	2.4	5.0	94.9	97.5	99.1
	R_l^c	1.1	2.7	5.3	94.3	97.2	99.0
	R_{ls}^c	1.0	2.5	5.0	94.9	97.5	99.1
Beta	R	0.0	0.0	0.0	10.7	17.5	28.6
	R^*	0.8	2.2	4.6	94.4	97.2	99.0
	R^u	0.9	2.3	4.7	94.3	97.1	98.9
	R^c	0.9	2.4	4.9	94.7	97.2	99.0
	R_l^c	1.1	2.6	5.2	94.4	97.1	98.9
	R_{ls}^c	0.9	2.4	4.9	94.7	97.4	99.0
Curved exponential family	R	40.6	54.4	66.0	100.0	100.0	100.0
	R^*	1.1	2.8	5.3	95.3	97.7	99.1
	R^u	0.8	2.1	4.1	95.2	97.6	99.0
	R^c	1.1	2.7	5.1	95.4	97.6	99.0
	R_l^c	1.2	3.0	5.8	94.9	97.4	98.8
	R_{ls}^c	1.1	2.7	5.2	95.3	97.6	99.0
Behrens-Fisher	R	2.1	4.6	8.0	92.9	96.0	97.8
	R^*	1.1	2.6	5.2	95.2	97.5	99.1
	R^u	1.0	2.5	5.1	95.4	97.6	99.1
	R^c	1.0	2.5	5.1	95.4	97.6	99.1
	R_l^c	2.1	4.5	8.0	92.8	95.9	97.9
	R_{ls}^c	1.0	2.5	5.2	95.4	97.5	99.1
Logistic regression	R	4.0	7.7	12.9	97.2	98.7	99.4
	R^*	1.1	2.5	5.3	94.9	97.5	99.0
	R^u	0.3	1.2	2.5	96.7	98.7	99.6
	R^c	1.1	2.5	5.3	94.9	97.5	99.0
	R_l^c	1.6	3.5	6.4	93.8	96.6	98.5
	R_{ls}^c	1.1	2.6	5.3	94.9	97.5	99.0

Table S8: Empirical tail probabilities $\times 100$ for the statistics in Table 1 of the main text and all models that have been considered in the simulation experiments. The figures shown have been rounded to 1 decimal and are for $q = 100$ and $m = 16$.

Model	Statistic	Nominal					
		1.0	2.5	5.0	95.0	97.5	99.0
Gamma	R	0.0	0.0	0.1	48.7	61.2	73.7
	R^*	1.2	2.7	5.3	94.9	97.4	99.0
	R^u	1.2	2.8	5.5	95.1	97.7	99.0
	R^c	1.2	2.7	5.4	95.0	97.6	99.1
	R_l^c	1.3	2.9	5.7	94.8	97.5	99.0
	R_{ls}^c	1.3	2.8	5.5	95.1	97.6	99.1
Beta	R	0.0	0.0	0.0	34.8	47.2	61.1
	R^*	0.9	2.3	4.7	94.7	97.4	98.9
	R^u	1.0	2.3	4.6	94.7	97.3	98.9
	R^c	0.9	2.2	4.7	94.8	97.4	98.9
	R_l^c	1.0	2.4	4.9	94.5	97.4	98.9
	R_{ls}^c	1.0	2.4	4.8	94.8	97.4	98.9
Curved exponential family	R	19.0	30.3	42.2	99.9	100.0	100.0
	R^*	1.0	2.6	5.5	95.3	97.5	99.0
	R^u	0.8	2.3	4.9	95.2	97.6	99.0
	R^c	0.9	2.6	5.4	95.2	97.5	99.0
	R_l^c	1.1	2.8	5.6	95.0	97.4	98.9
	R_{ls}^c	1.0	2.6	5.4	95.2	97.5	99.0
Behrens-Fisher	R	1.7	3.6	6.6	93.4	96.4	98.4
	R^*	1.2	2.8	5.4	94.6	97.4	98.9
	R^u	1.1	2.8	5.3	94.6	97.4	98.9
	R^c	1.1	2.7	5.3	94.6	97.4	98.9
	R_l^c	1.7	3.6	6.7	93.3	96.4	98.4
	R_{ls}^c	1.1	2.9	5.4	94.5	97.4	98.9
Logistic regression	R	2.7	5.9	10.0	97.0	98.6	99.4
	R^*	1.1	2.8	5.5	95.0	97.6	99.1
	R^u	0.7	1.9	4.2	96.0	98.2	99.3
	R^c	1.1	2.8	5.6	95.1	97.6	99.0
	R_l^c	1.4	3.2	6.2	94.5	97.2	98.9
	R_{ls}^c	1.1	2.8	5.5	95.0	97.6	99.1

Table S9: Empirical tail probabilities $\times 100$ for the statistics in Table 1 of the main text and all models that have been considered in the simulation experiments. The figures shown have been rounded to 1 decimal and are for $q = 1000$ and $m = 4$.

Model	Statistic	Nominal					
		1.0	2.5	5.0	95.0	97.5	99.0
Gamma	R	0.0	0.0	0.0	0.0	0.0	0.0
	R^*	0.2	0.5	1.2	83.7	90.3	95.3
	R^u	1.3	3.2	6.4	96.4	98.2	99.2
	R^c	1.0	2.5	5.1	94.8	97.4	98.9
	R_l^c	1.4	3.1	6.2	93.9	96.7	98.5
	R_{ls}^c	1.0	2.5	5.1	95.0	97.4	98.9
Beta	R	0.0	0.0	0.0	0.0	0.0	0.0
	R^*	0.3	0.8	1.8	88.6	93.5	96.7
	R^u	0.5	1.3	2.8	91.4	94.9	97.6
	R^c	0.7	1.9	3.8	93.7	96.4	98.6
	R_l^c	1.0	2.3	4.6	92.9	95.7	98.1
	R_{ls}^c	0.8	1.8	3.9	93.7	96.5	98.5
Curved exponential family	R	100.0	100.0	100.0	100.0	100.0	100.0
	R^*	3.2	6.3	10.6	97.8	99.0	99.6
	R^u	0.4	1.3	2.7	92.8	96.4	98.5
	R^c	2.2	4.8	8.3	96.9	98.5	99.4
	R_l^c	3.1	6.0	9.8	96.2	98.0	99.2
	R_{ls}^c	2.4	4.9	8.3	96.9	98.6	99.4
Behrens-Fisher	R	5.3	8.7	12.3	87.8	92.0	95.1
	R^*	1.5	3.3	6.3	94.1	96.8	98.6
	R^u	1.0	2.6	5.2	95.1	97.5	99.0
	R^c	1.0	2.7	5.1	95.1	97.5	99.1
	R_l^c	5.3	8.7	12.3	87.8	92.0	95.1
	R_{ls}^c	1.1	2.7	5.1	95.1	97.4	99.0
Logistic regression	R	40.2	53.2	64.3	99.9	100.0	100.0
	R^*	2.0	4.5	8.3	97.1	98.5	99.5
	R^u	0.0	0.1	0.5	97.2	98.9	99.8
	R^c	1.8	4.2	8.1	97.0	98.5	99.4
	R_l^c	3.7	7.5	11.8	95.2	97.3	98.7
	R_{ls}^c	1.8	4.2	8.2	97.0	98.5	99.5

Table S10: Empirical tail probabilities $\times 100$ for the statistics in Table 1 of the main text and all models that have been considered in the simulation experiments. The figures shown have been rounded to 1 decimal and are for $q = 1000$ and $m = 8$. The first 4 blocks of rows are identical to Table 2 of the main text.

Model	Statistic	Nominal					
		1.0	2.5	5.0	95.0	97.5	99.0
Gamma	R	0.0	0.0	0.0	0.0	0.0	0.0
	R^*	0.7	1.5	3.3	92.1	95.5	98.2
	R^u	1.1	2.7	5.3	95.1	97.7	99.2
	R^c	1.0	2.5	5.0	94.6	97.2	99.0
	R_l^c	1.1	2.8	5.4	94.2	96.8	98.9
	R_{ls}^c	1.1	2.5	4.9	94.5	97.2	99.1
Beta	R	0.0	0.0	0.0	0.0	0.0	0.0
	R^*	0.7	1.8	3.8	93.7	96.8	98.8
	R^u	0.8	1.9	4.1	94.0	97.0	98.7
	R^c	1.0	2.3	4.8	95.0	97.4	99.1
	R_l^c	1.1	2.5	5.1	94.7	97.3	98.9
	R_{ls}^c	0.9	2.3	4.8	95.1	97.5	99.0
Curved exponential family	R	100.0	100.0	100.0	100.0	100.0	100.0
	R^*	1.4	3.5	6.9	96.6	98.3	99.4
	R^u	0.6	1.8	4.0	95.0	97.7	99.2
	R^c	1.2	3.3	6.4	96.2	98.2	99.4
	R_l^c	1.5	3.6	7.1	95.8	98.0	99.2
	R_{ls}^c	1.3	3.2	6.5	96.3	98.2	99.4
Behrens-Fisher	R	2.4	4.6	7.6	92.1	95.6	98.0
	R^*	1.2	2.8	5.3	94.8	97.5	99.0
	R^u	1.1	2.7	5.2	95.0	97.6	99.1
	R^c	1.1	2.7	5.1	94.9	97.6	99.1
	R_l^c	2.4	4.7	7.6	92.1	95.5	98.0
	R_{ls}^c	1.1	2.6	5.1	95.0	97.6	99.1
Logistic regression	R	18.1	28.4	39.3	99.7	99.9	100.0
	R^*	1.4	3.1	6.1	95.8	97.9	99.1
	R^u	0.4	1.1	2.4	96.3	98.4	99.4
	R^c	1.5	3.1	6.0	95.8	97.9	99.2
	R_l^c	1.9	4.1	7.5	94.7	97.1	98.8
	R_{ls}^c	1.4	3.2	6.0	95.8	97.9	99.1

Table S11: Empirical tail probabilities $\times 100$ for the statistics in Table 1 of the main text and all models that have been considered in the simulation experiments. The figures shown have been rounded to 1 decimal and are for $q = 1000$ and $m = 16$.

Model	Statistic	Nominal					
		1.0	2.5	5.0	95.0	97.5	99.0
Gamma	R	0.0	0.0	0.0	0.0	0.0	0.2
	R^*	0.9	2.1	4.3	94.3	96.9	98.5
	R^u	1.1	2.5	5.0	95.2	97.6	98.9
	R^c	1.0	2.5	4.9	95.0	97.5	98.9
	R_l^c	1.1	2.6	5.1	94.8	97.3	98.6
	R_{ls}^c	1.1	2.5	5.0	95.0	97.5	98.8
Beta	R	0.0	0.0	0.0	0.0	0.0	0.0
	R^*	1.0	2.3	4.5	94.3	97.2	98.8
	R^u	1.1	2.3	4.7	94.4	97.2	98.8
	R^c	1.0	2.4	4.8	94.8	97.4	99.0
	R_l^c	1.2	2.5	5.0	94.7	97.3	98.9
	R_{ls}^c	1.1	2.4	4.9	94.8	97.4	98.9
Curved exponential family	R	98.2	99.3	99.7	100.0	100.0	100.0
	R^*	1.0	2.8	5.5	95.9	98.1	99.3
	R^u	0.7	2.1	4.5	95.3	97.9	99.3
	R^c	1.1	2.6	5.4	95.7	98.1	99.3
	R_l^c	1.1	2.8	5.7	95.5	97.9	99.2
	R_{ls}^c	1.0	2.6	5.4	95.7	98.0	99.3
Behrens-Fisher	R	1.5	3.4	6.1	93.9	96.6	98.5
	R^*	1.1	2.6	5.0	94.9	97.5	98.9
	R^u	1.1	2.6	5.0	95.0	97.5	99.1
	R^c	1.1	2.6	5.0	95.1	97.5	99.1
	R_l^c	1.5	3.4	6.2	93.8	96.7	98.5
	R_{ls}^c	1.1	2.6	4.9	95.0	97.5	99.0
Logistic regression	R	8.5	15.2	23.7	99.3	99.7	100.0
	R^*	1.3	2.9	5.5	95.1	97.7	99.0
	R^u	0.7	1.9	3.9	95.5	98.0	99.2
	R^c	1.3	2.9	5.5	95.1	97.6	99.0
	R_l^c	1.6	3.4	6.0	94.7	97.2	98.9
	R_{ls}^c	1.3	2.9	5.5	95.1	97.6	99.1